scientific reports

Check for updates

OPEN

Scythicorhinus vekuai gen. nov. et comb. nov. (Mammalia, Rhinocerotidae) from the Pliocene of Georgia and its implications for the early evolution of *Coelodonta* and *Stephanorhinus*

Oleksandr Kovalchuk[1,2]✉, Antonio Borrani[3], Paweł Mackiewicz[4], Zoltán Barkaszi[1,5], Chiara Capalbo[6], Svitozar Davydenko[7], Anastasiia Dubikovska[1,7,8], Urszula Ratajczak-Skrzatek[2], Maxim Sinitsa[9], Krzysztof Stefaniak[2], Maciej T. Krajcarz[10] & Paul P. A. Mazza[6]

The taxonomy of Eurasian rhinoceroses has long been complicated by extensive homoplasy, incomplete fossil records, and shifting diagnostic criteria, particularly affecting the genera *Dicerorhinus*, *Dihoplus*, *Pliorhinus*, *Rhinoceros*, and *Stephanorhinus*. Rhinocerotid material from the Late Pliocene locality of Kvabebi (Georgia), previously referred to *Pliorhinus miguelcrusafonti*, is re-evaluated here using an expanded morphological dataset and phylogenetic analyses. The results consistently recover the Kvabebi rhinoceros as a distinct dicerorhinine lineage positioned close to the divergence between *Coelodonta* and *Stephanorhinus*. On the basis of its unique combination of cranial, dental, and postcranial characters, and its stable phylogenetic placement outside both *Coelodonta* and *Stephanorhinus*, the Kvabebi material is provisionally assigned to *Scythicorhinus vekuai* (Tsiskarishvili, 1987) gen. nov. et comb. nov. Although alternative placements within the early *Coelodonta–Stephanorhinus* radiation cannot be statistically rejected, a close relationship with *Stephanorhinus miguelcrusafonti* is strongly unsupported. Two fragmentary maxillae from Berehove (Crimea, Ukraine) are also examined and are tentatively referred to *Scythicorhinus vekuai*, pending the discovery of more diagnostic material. Discrete-character and morphometric analyses indicate that both the Kvabebi and Berehove rhinoceroses fall outside the observed morphological variation of *Coelodonta* and *Stephanorhinus*, supporting their distinction at the generic level, albeit provisionally given the limited and partially worn material. The results further support rejection of *Pliorhinus* as a valid genus. Overall, this study refines the systematic framework of late Neogene rhinocerotids and underscores the importance of expanded comparative datasets for resolving evolutionary relationships within this highly homoplastic group.

The subfamily Rhinocerotinae encompasses all living rhinoceroses as well as a diverse array of extinct relatives, representing a major lineage of Cenozoic megaherbivores[1–4]. Although only five extant species persist today—the Indian rhinoceros *Rhinoceros unicornis*, the Javan rhinoceros *Rhinoceros sondaicus*, the Sumatran rhinoceros

[1]National Museum of Natural History of the National Academy of Sciences of Ukraine, Kyiv, Ukraine. [2]Department of Palaeozoology, University of Wrocław, Wrocław, Poland. [3]Soprintendenza Archeologia, Belle Arti e Paesaggio per le Province di Frosinone e Latina, Latina, Italy. [4]Department of Bioinformatics and Genomics, University of Wrocław, Wrocław, Poland. [5]Department of Agricultural Sciences, John Von Neumann University, Kecskemét, Hungary. [6]Department of Earth Sciences, University of Florence, Florence, Italy. [7]Schmalhausen Institute of Zoology, National Academy of Sciences of Ukraine, Kyiv, Ukraine. [8]A. S. Makarenko Sumy State Pedagogical University, Sumy, Ukraine. [9]Dipartimento Di Scienze, Università Roma Tre, Rome, Italy. [10]GeoEco Research Group, Institute of Geological Sciences, Polish Academy of Sciences, Warsaw, Poland. ✉email: biologiest@ukr.net

Dicerorhinus sumatrensis, the white rhinoceros *Ceratotherium simum*, and the black rhinoceros *Diceros bicornis*—the fossil record reveals that rhinocerotids were once far more taxonomically and ecologically diverse, occupying a wide range of environments across Eurasia[5–8]. Despite extensive research, the taxonomy and evolutionary history of Neogene and Quaternary Eurasian rhinoceroses remain incompletely resolved[6,7,79]. Persistent uncertainty is driven by frequent homoplasy, incomplete fossil records, and shifting diagnostic criteria, which have led to repeated revisions and ongoing debates regarding the classification of several key genera, including *Rhinoceros*, *Dicerorhinus*, *Stephanorhinus*, *Dihoplus*, and *Pliorhinus*.

A notable example is *Rhinoceros megarhinus* De Christol, 1834, whose generic placement has fluctuated among *Rhinoceros*[9], *Dicerorhinus*[10], *Stephanorhinus*[11,12] and more recently *Dihoplus*, owing to a combination of cranial and dental characters (e.g., nasal septum not ossified, loss of anterior teeth) that does not conform to traditional generic diagnoses. Consequently, numerous morphological reinterpretations of this lineage have been proposed over decades[13–20]. Similar instability affects *Dicerorhinus miguelcrusafonti* Guérin and Santafé-Llopis, 1978, whose taxonomic status has also shifted repeatedly. These difficulties highlight the need for broader comparative datasets and more inclusive phylogenetic frameworks to clarify the early evolution of the *Stephanorhinus–Coelodonta* lineage. Historical binomials (e.g., *Rhinoceros megarhinus*, *Dicerorhinus miguelcrusafonti*) are used only when referring to taxonomic history; throughout this study, the combinations *Stephanorhinus megarhinus* and *Stephanorhinus miguelcrusafonti* are used. Pandolfi et al.[13,14] noted morphological similarities between the Late Pliocene rhinoceros remains from Kvabebi (Georgia) and material from Layna (Spain) and Perpignan (France), previously described as *Dicerorhinus miguelcrusafonti*[15], *Stephanorhinus miguelcrusafonti*[16,19] or *Dihoplus miguelcrusafonti*[20]. On this basis, the Kvabebi assemblage was referred to the same species and, together with *Dihoplus megarhinus*, assigned to the newly erected genus *Pliorhinus*[13,19]. Later studies further expanded *Pliorhinus* to include *Dihoplus ringstroemi*[21]. However, the validity and monophyly of *Pliorhinus* have recently been questioned[22], and the phylogenetic position of the Kvabebi rhinoceros within *Stephanorhinus* remains insufficiently resolved. The Kvabebi assemblage, being among the well-preserved Late Pliocene rhinoceroses from the southern margin of Eastern Europe, represents a key case study for evaluating early *Stephanorhinus* evolution.

The aim of this study is to reassess the Kvabebi rhinoceros within an expanded morphological and phylogenetic framework and to determine whether it represents an undescribed taxon. Cladistic, morphometric, and character-based phylogenetic analyses consistently recover the Kvabebi material as a distinct taxon, herein named *Scythicorhinus vekuai* gen. nov. et comb. nov., placed basally within the *Coelodonta* clade, close to the node uniting *Coelodonta* and *Stephanorhinus*. Additional material from Berehove (Crimea, Ukraine) was examined within the same analytical framework and tentatively referred to this species. By clarifying the systematic position of the Kvabebi rhinoceros and evaluating the affinities of the Berehove specimens, this study provides new insights into the early evolution of the *Coelodonta* and *Stephanorhinus* lineage in Eastern Europe—a region that may have played a role in its early diversification, although this hypothesis is not directly tested here. These results refine the systematic framework of late Neogene dicerorhinines and clarify character evolution near the *Coelodonta–Stephanorhinus* divergence.

Kvabebi locality and material

The fossil assemblage from Kvabebi (eastern Georgia) was first described by Vekua[23] and Tsiskarishvili[24]. Later, it was re-evaluated by Pandolfi et al.[13] during their revision of northern Eurasian rhinocerotines, constituting one of the most complete Late Pliocene rhinoceros records from the southern margin of Eastern Europe. In the material currently available for study, alongside two partial crania, an associated mandible with p3–m3, there are isolated permanent and deciduous teeth, and a broad array of postcranial elements. However, earlier descriptions and illustrations (Vekua[23]; Tsiskarishvili[24]: pl. XXVII) clearly document the presence of p2 in the Kvabebi assemblage, indicating that the anterior portion of the dentition was originally present but is no longer preserved or accessible in the currently available material. All specimens from Kvabebi (GNM1 29-2013) are curated in the Simon Janashia Museum of Georgia, Georgian National Museum, Tbilisi (GNM). Although some bones show partial crushing, the assemblage preserves an unusually rich combination of cranial, mandibular, and postcranial structures allowing a robust assessment of taxonomic identity. Pandolfi et al.[13] regarded the Kvabebi rhinoceros as conspecific with "*Dicerorhinus*" *miguelcrusafonti* from Layna and Perpignan, and used these occurrences collectively to establish the genus *Pliorhinus*. However, aspects of their classification—including limited character sampling, a narrow outgroup selection and reliance on frequency-based traits—leave the phylogenetic placement of the Kvabebi material open to re-evaluation under a broader and more inclusive morphological and cladistic framework. The cranial morphology, P2–M3 dental pattern, mandibular ramus structure, and the configuration of the radius, ulna, tibia, and astragalus together form a coherent suite of characters not observed in any known *Stephanorhinus* species, nor in the combinations reported for *Dihoplus* or *Pliorhinus*. Instead, these features consistently place the Kvabebi rhinoceros as an early-branching member of the *Coelodonta* lineage. Given its anatomical completeness and its central role in the phylogenetic signal, the Kvabebi material constitutes the holotype and hypodigm of *Scythicorhinus vekuai* gen. nov. et comb. nov., and all diagnostic statements in this study are based exclusively on this assemblage.

Berehove locality and material

The Berehove locality is situated on the Black Sea coast, approximately 2 km north of the eponymous village in the Bakhchysarai District, southwestern Crimea, Ukraine (Fig. 1). Fossil rhinoceros remains were discovered in 1962 by Ye. Ratekhin within loams overlain by 8 m of yellow–brown clays with loam lenses[25]. These sediments belong to the Tauris Formation[26] (=Tavrska suite in the State Geological Map of Ukraine[27]) within the Alma structural-facies zone[28]. The formation correlates with the upper Kimmerian and Kuyalnikian stages[26,29] and corresponds to the upper Zanclean and lower Piacenzian[30] (Early–Late Pliocene transition, ca. 4.2–3.5 Ma; MN

Fig. 1. Schematic map indicating the geographic placement of the studied localities.

15). Associated large-mammal fossils from this site include teeth of *Anancus* aff. *A. arvernensis*[31], a metatarsal of *Hipparion elegans*, and a tusk and molar tooth of *Tetralophodon* aff. *T. longirostris*[32,33]. The studied material consists of two fragmentary maxillae of a large rhinoceros: a partial right maxilla with P2–M3, and a fragmentary left maxilla with P2–P4. Both specimens are housed in the National Museum of Natural History, National Academy of Sciences of Ukraine, Kyiv (NMNHU-P UN 1501). The closely matching tooth dimensions and wear patterns (wear stage 6/7 after Kaiser et al.[34]), together with their proximity of discovery, suggest that the two maxillae most likely derive from a single individual. Advanced dental wear and the limited set of preserved characters, however, render the Berehove material undiagnostic at the species level. Despite these limitations, the morphology and proportions of the Berehove maxillae show no conflict with those of *Scythicorhinus vekuai* gen. nov. et comb. nov. Consequently, these specimens are treated as tentatively referable to this species, pending the discovery of more complete material.

Systematic paleontology

Order Perissodactyla Owen, 1848

Superfamily Rhinocerotoidea Gray, 1821

Family Rhinocerotidae Gray, 1821

Subfamily Rhinocerotinae Gray, 1821

Tribe Rhinocerotini Gray, 1821

Subtribe Dicerorhinina Ringström, 1924

Type species: *Dicerorhinus sumatrensis* (Fischer, 1814)

Included genera: *Coelodonta*, *Dicerorhinus*, *Dihoplus*, *Stephanorhinus*, *Scythicorhinus* gen. nov.

Emended diagnosis: Members of Rhinocerotini in which the mental foramen lies anterior to p3; d1/p1 typically absent in adults; and d2 bears a paralophid.

Scythicorhinus gen. nov.

urn:lsid:zoobank.org:pub:1D545B85-EEBF-4292-9FED-DF4EF581E408

urn:lsid:zoobank.org:act:353929B6-E02D-44B9-B387-D4D792183BBB

Etymology: The generic name *Scythicorhinus* derives from "scythicus", referring to the Scythians — the ancient equestrian nomadic populations historically associated with the Pontic–Caspian steppe and the Caucasus region — combined with the Greek rhinos (ῥίς, ῥινός), meaning "nose" or "rhinoceros." The name emphasizes both the geographic context of the type locality (eastern Georgia, within the broader Scythian cultural-historical corridor) and the phylogenetic distinctiveness of this rhinocerotid lineage. The gender of the name is masculine.

Type species: Scythicorhinus vekuai (Tsiskarishvili, 1987) comb. nov.

Diagnosis: same as for the type and only species.

Scythicorhinus vekuai (Tsiskarishvili, 1987) comb. nov.

urn:lsid:zoobank.org:act:25E9488E-8362-47EA-A757-DF39C09F89D5.

Dicerorhinus megarhinus (Christol): Vekua, 1972, pp. 161–181, figs. 34–43, pl. XXII–XXVI.

Dicerorhinus vekuai sp. nov.: Tsiskarishvili, 1987, pp. 81–91, pl. XXVI–XXVII.

Pliorhinus miguelcrusafonti (Guérin & Santafe-Llopis, 1978): Pandolfi et al., 2021 (partim; misidentification).

Pliorhinus miguelcrusafonti (Guérin & Santafe-Llopis, 1978): Pandolfi et al., 2022 (partim; misidentification).

Holotype: GNM1 29-2013/925 DN-229, neurocranial portion of skull from Kvabebi (Georgia), housed in the Simon Janashia Museum of Georgia, Georgian National Museum, Tbilisi.

Hypodigm: GNM1 29-2013/925, crushed skull bearing right P2–M3; GNM1 29-2013/925, horizontal ramus of mandible bearing p3–m3; GNM1 29-2013/278, fragment of left mandible bearing p3 and p4; GNM1 29-2013/288 (K86), left M3; GNM1 29-2013/290 (K85), right P4; GNM1 29-2013/286 (K80), right D3; GNM1 29-2013/285 (K75), right D4; GNM1 29-2013/287 (K79), right D4; GNM1 29-2013/284 (K88-K89), right M2–M3; GNM1 29-2013/282 (K905), right d3; GNM1 29-2013/279 (K82), right m3; GNM1 29-2013/270 (K760), proximal epiphysis of left radius with fragment of ulna; GNM1 29-2013/271 (K355 or K399), fragment of right distal epiphysis of radius and ulna; GNM1 29-2013/273 (K753), almost complete left ulna; GNM1 29-2013/274 (K505), distal epiphysis of left tibia; GNM1 29-2013/275 (K71), proximal epiphysis of right Mt3; GNM1 29-2013/276, proximal epiphysis of right radius; GNM1 29-2013/277 (K65), damaged first lateral phalanx; GNM1 29-2013/292 (K492), mesiolingual fragment of right upper premolar; GNM1 29-2013/293 (K81), fragment of protocone of left upper deciduous; GNM1 29–2013/294 (K493), fragment of upper premolar; GNM1 29-2013/295 (K500), lingual fragment of lower molar; GNM1 29-2013/296 (K496), fragment of upper tooth; GNM1 29-2013/297 (K497), vestibular fragment of right upper molar; GNM1 29-2013/302 (K767), right humerus; GNM1 29-2013/342 (K61), left scaphoid; GNM1 29-2013/343 (K70), left unciform; GNM1 29-2013/344 (K53), left unciform; GNM1 29-2013/345 (K74), fragment of left magnum; GNM1 29-2013/347 (K63), fragment of magnum; GNM1 29-2013/348 (K908), right semilunar; GNM1 29-2013/349 (K67), left pyramidal; GNM1 29-2013/350 (K60), left trapezoid; GNM1 29-2013/496 (K426), lingual fragment of left (second?) upper deciduous; GNM1 29-2013/537 (K3047), proximal fragment of right femur; GNM1 29-2013/539, distal fragment of right humerus; GNM1 29-2013/541 (K4240), fragment of diaphysis of radius; GNM1 29-2013/542 (K3068), fragment of long bone; GNM1 29-2013/631 (K3042), proximal fragment of left calcaneus; GNM1 29-2013/720 (K4467), fragment of humerus; GNM1 29-2013/752 (K533), right tibia; GNM1 29-2013/756 (K69), left calcaneus; GNM1 29-2013/758 (K72), right Mc3; GNM1 29-2013/759 (K64), left Mc2; GNM1 29-2013/760, fragment of long bone; GNM1 29-2013/761 (K901), right astragalus; GNM1 29-2013/766 (K3106), fragment of diaphysis of right humerus; GNM1 29–2013/929 (K759), proximal fragment of left ulna; GNM1 29-2013/930 (K737), fragment of femur; GNM1 29-2013/931, proximal fragment of humerus; GNM1 29-2013/933 (K66), distal fragment of left Mt3; GNM1 29-2013/934 (K73), proximal fragment of right Mt4; GNM1 29-2013/281 (K84), worn left lower molar; NMNHU-P UN 1501/1, partial right maxilla with P2–M3; NMNHU-P UN 1501/2, fragmentary left maxilla with P2–P4. All elements of the Kvabebi assemblage designated as the holotype and hypodigm were illustrated by Pandolfi et al.[13]. As the present study re-examines exactly the same specimens, those published figures serve as the definitive visual documentation of the type material and enable independent assessment of its morphology.

Specimens reported by Vekua[23] but absent in the collection of the Simon Janashia Museum of Georgia are as follows: K525, fragment of fibula (pp. 161, 173); K495, P2 (pp. 161, 164); K77, left D3 (pp. 161–163, pl. XXIII, Fig. 2); K78, left D2 (pp. 161–163, pl. XXIII, Fig. 2); K78, left D4 (pp. 161–163, pl. XXIII, Fig. 2); K62, trapezium (p. 169); K902, navicular (pp. 161, 174).

Geographic and chronological distribution: Kvabebi, eastern Georgia, latest Pliocene (ca. 2.864 ± 0.008 – 2.59 Ma[35]); Berehove, Ukraine, late Zanclean/earliest Piacenzian (4.2–3.5 Ma).

Diagnosis: A Dicerorhinina characterized by the following combination of characters: infraorbital foramen positioned beneath the lower rim of the orbit; external auditory pseudomeatus directed upwards and outwards; anterior facet of the postglenoid process convex with a median ridge; prominent occipital nuchal tubercle; mandibular foramen situated above the collar line; upper cheek teeth with a lingually curved outline, lacking labial and lingual cingula, P2 without a protoloph, P3–P4 with multiple crochets, and P4 showing distal-only constriction; M1 with fused protocone–hypocone bases, M2 with a weak parastyle fold, M3 lacking a posterior cingulum; deciduous lower teeth with a constricted metaconid (d2–d3), external vertical rugosity (d3), and entoconid constriction (d3). Humerus with a deep distal gutter on the epicondyle and a pronounced epicondylar crest; radius with a shallow insertion for *musculus biceps brachii*; tibia with the lateral intercondyloid eminence higher than the medial; posterior tibial apophysis inconspicuous; astragalus with nearly equal proximal–distal extension of the medial and lateral lips and a weak medio-distal tuberosity; calcaneus with a narrowly elongate second astragalar facet.

The reconstruction of the skull based on the Kvabebi sample is shown in Fig. 3. Some of the most relevant diagnostic characters are illustrated in Fig. 4.

Differential diagnosis: A genus of Dicerorhinina distinguished from both *Coelodonta* and *Stephanorhinus* by a unique combination of cranial, dental, and postcranial characters.

Differs from *Coelodonta* in:

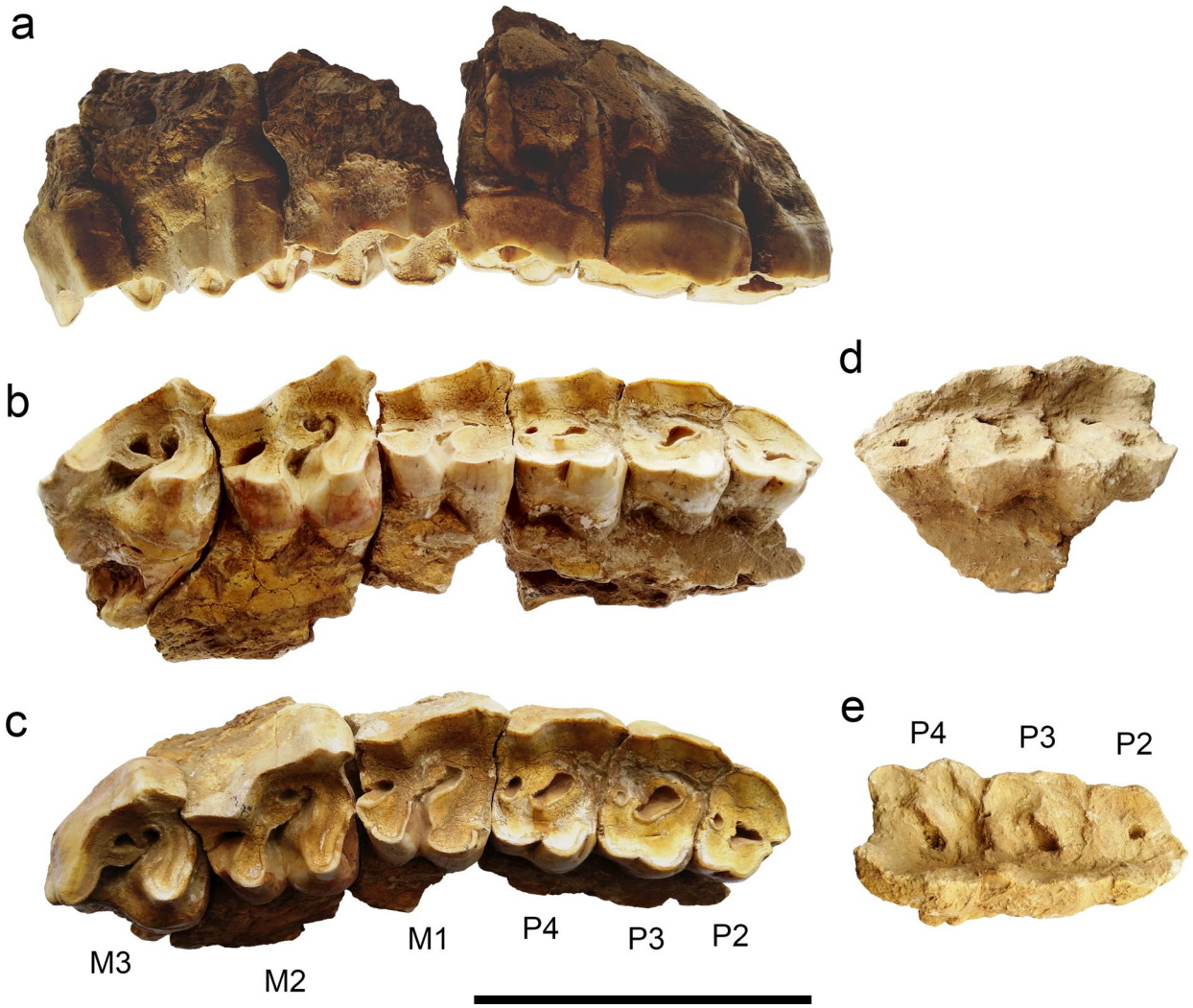

Fig. 2. Remains of the Berehove rhinoceros: (**a**–**c**) – right maxilla NMNHU-P UN-1501/1 in labial (**a**), lingual (**b**), and occlusal view (**c**); (**d**,**e**) – fragment of left maxilla NMNHU-P UN-1501/2 in lingual (**d**) and occlusal (**e**) views. Scale bar: 10 cm.

(1)Absence of the derived hypsodont and cement-covered dentition typical of *Coelodonta* (teeth mesodont and lacking cementum);

(2)Less derived enamel folding pattern, without complex plication;

(3)Presence of a lingually open medifossette on P4 (closed in *Coelodonta*);

(4)Same position of foramen infraorbitale relative to lower orbital rim (lower in *Coelodonta*);

(5)Concave outline of occipital crest in dorsal view (straight in *Coelodonta*);

(6)Absent crista on M1 (present in *Coelodonta*);

(7)More primitive postcranial morphology, including:

i. calcaneus with elongate but not highly specialized articular facets;
ii. generally smaller and less robust skeletal proportions relative to *Coelodonta*.Differs from *Stephanorhinus* in:

(1)Fusion of protocone and hypocone bases on M1 (separated in *Stephanorhinus*);

(2)Gently curved lingual outline of upper cheek teeth (typically straighter in *Stephanorhinus*);

(3)Distinct configuration of postcranial elements, including:

i. narrow distal ulna with deep extensor groove;
ii. lateral tibial intercondylar eminences higher than medial (equal in *Stephanorhinus*);
iii. less derived astragalus with nearly equal proximal–distal extension of medial and lateral lips (lateral lip longer than medial lip in *Stephanorhinus*) and weak medio-distal tuberosity (prominent in *Stephanorhinus*);

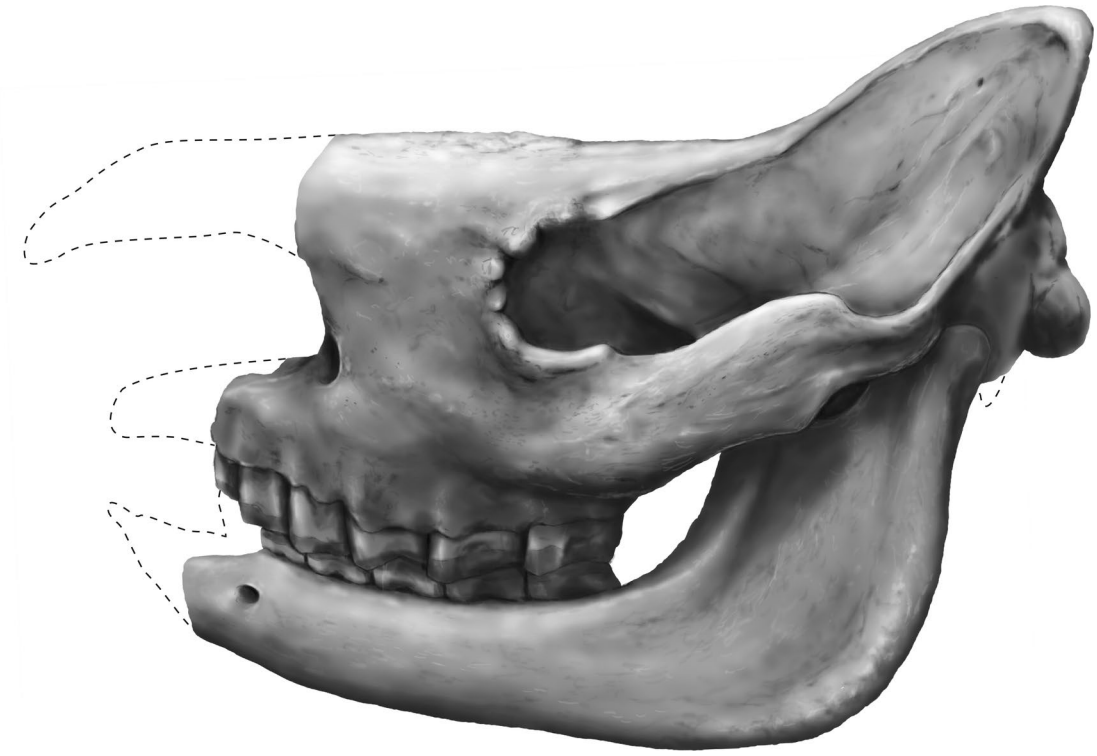

Fig. 3. Reconstruction of the skull of *Scythicorhinus vekuai* gen. nov. et comb. nov. Not to scale.

iv. shallow insertion of *musculus biceps brachii* (slightly protruding in *Stephanorhinus*).Differs from most representatives of both genera in (Table S1):

(1)Unique mosaic combination of primitive and derived traits;

(2)Consistent absence of lingual cingula on upper molars combined with fusion of lingual cusps on M1;

(3)Absence of posterior cingulum on M3;

(4)Strong crochet development (multiple crochet) on P4;

(5)Combination of dental and postcranial features not observed jointly in any species of *Coelodonta* or *Stephanorhinus*.

Taxonomic remarks

The genus *Pliorhinus* was established by Pandolfi et al.[13] to include "*Dihoplus*" *megarhinus* and the Kvabebi rhinoceros, interpreted as closely related taxa. Subsequent analyses[22] have shown that *megarhinus* is nested within *Stephanorhinus*, rendering *Pliorhinus* non-monophyletic and therefore unsupported as a distinct genus. In this context, the Kvabebi rhinoceros cannot be accommodated within *Pliorhinus*, as the type species of that genus (*P. megarhinus*) belongs to *Stephanorhinus*, and genus-group names are anchored to their type species. At the same time, the morphological and phylogenetic evidence presented here indicates that the Kvabebi material does not fit within the current diagnoses of either *Stephanorhinus* or *Coelodonta*. Accordingly, the Kvabebi rhinoceros is provisionally interpreted as representing a distinct lineage, for which the new genus *Scythicorhinus* is proposed in accordance with the International Code of Zoological Nomenclature[75]. This taxonomic interpretation is presented as a working hypothesis based on the available evidence and may be subject to revision with the discovery of additional material or further refinement of phylogenetic datasets.

Description of the Kvabebi rhinoceros

The Kvabebi material preserves an unusually complete anatomical set, including a crushed cranium with the right upper cheek-tooth row (P2–M3), isolated upper and lower cheek teeth, a mandible bearing p3–m3, deciduous teeth, and a diverse postcranial assemblage. The dental morphology is consistent with that described by Vekua[23], Tsiskarishvili[24] and by Pandolfi et al.[13] but, within the broader comparative framework applied here, clarifies several characters that were previously ambiguous. The upper cheek teeth are brachydont, with strongly folded enamel, deep valleys, and pronounced ectoloph ornamentation. The premolars are submolariform, proportionally shorter than the molars, and show a characteristic pattern of crista–crochet development. On P2, the ectoloph is convex and bears a prominent parastyle and a robust paracone rib; the protocone is moderately constricted, and a continuous lingual cingulum is absent. P3 and P4 display a small, lingually open medifossette and a crochet that may be simple or bifid, as noted by Pandolfi et al.[13]. A distal constriction is developed on P4.

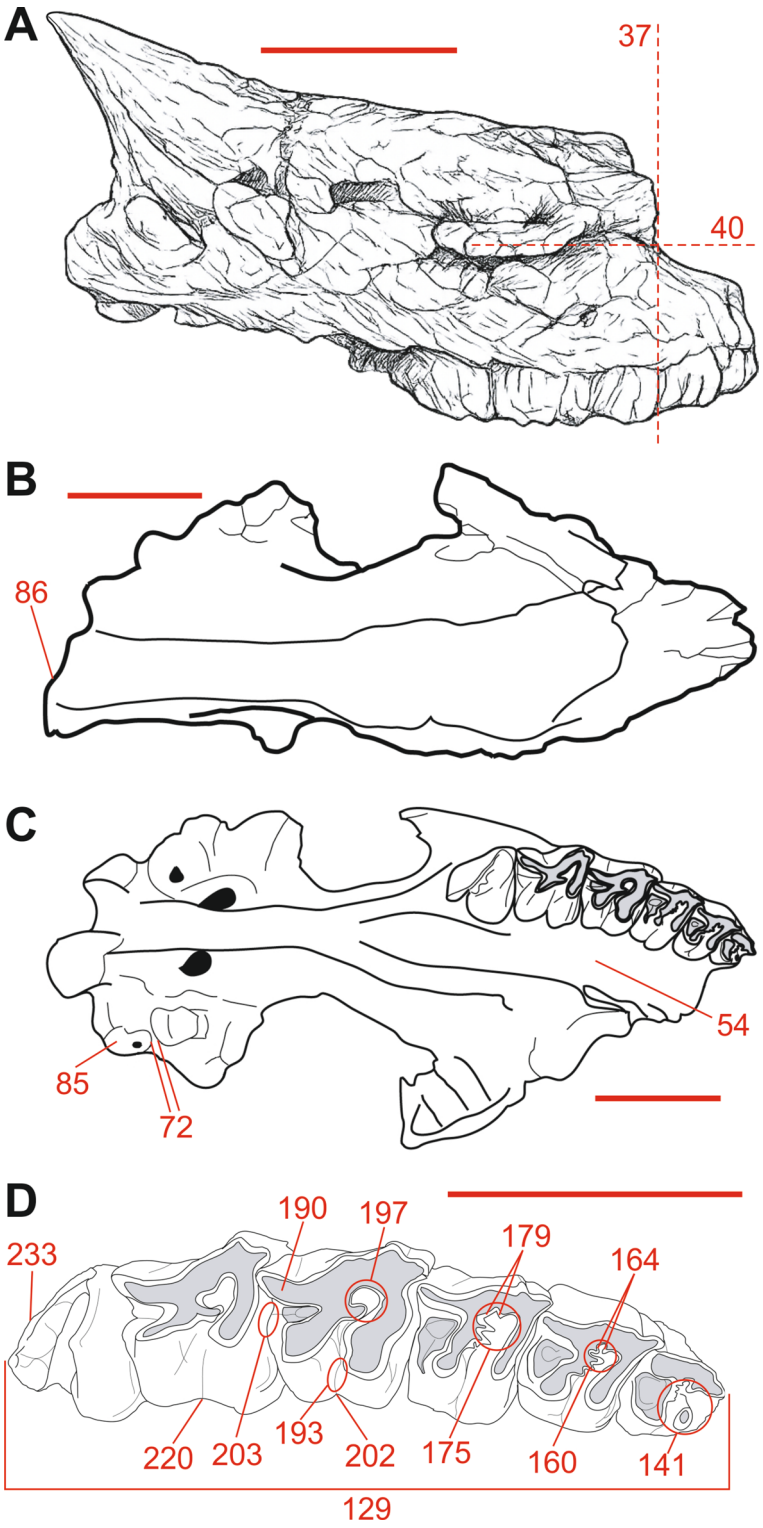

Fig. 4. Selected cranial and dental characters of *Scythicorhinus vekuai* gen. nov. et comb. nov. illustrating features that differentiate it from *Coelodonta* and/or *Stephanorhinus* (see Table S6 for full character-state distribution). Illustrated are the skull in lateral (**A**), dorsal (**B**) and ventral (**C**) views, and the upper cheek-tooth row in occlusal view (**D**). Scale bar: 10 cm.

The lingual outline of the cheek teeth is gently curved, contrasting with the straighter lingual profiles typical of *Dihoplus*.

The molars (M1–M3) exhibit strong development of the crochet and crista, which frequently fuse in advanced wear stages. On M1, the bases of the protocone and hypocone are fused, forming a continuous lingual structure

(character 193). This condition is shared with *Coelodonta* and differs from most species of *Stephanorhinus*, in which these cusps remain well separated. The fusion is clearly expressed even in moderate wear stages. The lingual cingulum is absent on the upper molars (character 220), and M3 lacks a posterior cingulum (character 233), a condition contrasting with its presence in both *Coelodonta* and most species of *Stephanorhinus*. The metacone fold is absent, as in *Stephanorhinus* species and *Coelodonta nihowanensis*, whereas it is present in three other species of *Coelodonta*. M2 bears a weak mesostyle. The protoloph of M3 is mesiodistally oriented, as in *Coelodonta* and *S. etruscus*, whereas in other species of *Stephanorhinus* it is transversely directed.

The lower dentition displays a combination of features characteristic of early members of the *Coelodonta–Stephanorhinus* lineage. On p3–p4, the metalophids are non-constricted and fused to the metaconid, and m1 shows complete fusion between the metaconid and a non-constricted metalophid—conditions typical of *Stephanorhinus* and not observed in *Dihoplus*. The preserved portion of the mandibular symphysis appears ventrally flat in frontal view; however, the incomplete preservation does not allow full reconstruction of the anterior symphyseal morphology.

Postcranially, the Kvabebi rhinoceros exhibits an M-shaped proximal articulation of the radius, an unexpanded distal ulna with a deep extensor groove, and a tibia with lateral intercondyloid eminence higher than the medial one. The astragalus shows nearly equal proximal–distal extension of the medial and lateral lips. The calcaneus bears an elongate proximodistal second facet and low sustentaculum calcanei. Together, these characters fall within the morphological range of *Stephanorhinus* but differ from the more derived configurations typical of *Coelodonta*, while also excluding attribution to *Dihoplus*. The cranial, mandibular, dental and postcranial characters of the Kvabebi rhinoceros form a coherent morphological suite that is incompatible with *Dihoplus* or *Pliorhinus* as defined by Pandolfi et al.[13]. Instead, these traits consistently position the Kvabebi material as an early-branching member of the *Coelodonta–Stephanorhinus* lineage, consistent with its interpretation as a distinct taxon, herein named *Scythicorhinus vekuai* gen. nov. et comb. nov.

Comparative assessment with Stephanorhinus miguelcrusafonti

Earlier attributions of the Kvabebi rhinoceros to *S. miguelcrusafonti* cannot be upheld when the full suite of cranial, dental, and postcranial characters is evaluated within the expanded comparative and phylogenetic framework applied here. The comparison is based on the diagnostic features and measurements described for the holotype and referred material of *S. miguelcrusafonti* by Guérin & Santafé-Llopis[36] and in the subsequent revision by Pandolfi et al.[13,14], including published illustrations of the relevant specimens. The characters used by Pandolfi et al.[13,14] to support conspecificity are either absent, reversed, or expressed in a different configuration in the Kvabebi material.

Several key inconsistencies emerge from direct comparison. In ventral view, the lingual outline of the upper cheek teeth is described as straight in *S. miguelcrusafonti*, whereas in the Kvabebi material it appears gently and consistently curved, forming a lingual concavity. Although minor post-mortem deformation cannot be entirely excluded, the curvature is expressed along the preserved tooth row and is not confined to areas showing visible crushing. A weak lingual cingulum is present on the upper molars of *S. miguelcrusafonti*, whereas no such structure is developed in the Kvabebi rhinoceros. On M2, *S. miguelcrusafonti* lacks a true medifossette sensu stricto; the structure present corresponds to a crochet that does not form a closed medifossette. In addition, it shows a non-constricted protocone, while both features are clearly expressed in the Kvabebi specimen. Postcranially, additional differences are observed in several basipodial elements. The scaphoid of the Kvabebi rhinoceros exhibits a quadrangular proximal facet (character 417), differing from the more rounded configuration described for *S. miguelcrusafonti*. The astragalus shows nearly equal proximal–distal extension of the medial and lateral lips, whereas in *S. miguelcrusafonti* the medial lip is more elongated. The calcaneus bears a narrowly elongate second astragalar facet and a relatively low sustentaculum calcanei, differing from the broader and more elevated morphology reported for *S. miguelcrusafonti*.

Description of the Berehove dentition

The upper cheek teeth of the Berehove rhinoceros (Fig. 2, Supplementary 3D, Tables 1 and 2) closely match the morphological pattern typical of *Coelodonta* and *Stephanorhinus* species[37]. They are brachydont, with wrinkled enamel and no cementum.

The premolar row is distinctly shorter than the molar row (Table 1), and the premolars are submolariform but retain relatively simple occlusal morphology. In particular, the protocone is weakly connected to the ectoloph

Measurement	Right	Left
Premolar (P2-P4) length (occlusal, labial view)	118.2	114.0
Premolar (P2-P4) length (at the base of crowns, labial view)	116.7	106.3
Premolar (P2-P4) length (occlusal, lingual view)	116.0	101.6
Premolar (P2-P4) length (at the base of crowns, lingual view)	111.1	90.7
Molar (M1-M3) length (occlusal, labial view)	153.3	–
Molar (M1-M3) length (at the base of crowns, labial view)	167.9	–
Molar (M1-M3) length (occlusal, lingual view)	142.9	–
Molar (M1-M3) length (at the base of crowns, lingual view)	149.4	–

Table 1. Maxillary dentition measurements (mm) of the Berehove rhinoceros.

Tooth	Side	DAP_0	DAPb	DTa	DTp	HIi
P2	Left	37.3	38.2	37.1	42.7	–
P3	Left	43.0	44.0	52.4	49.8	–
P4	Left	41.4	-	56.2	48.3	–
P2	Right	37.7	37.8	39.5	45.1	9.1
P3	Right	42.6	42.8	56.1	54.2	11.0
P4	Right	44.5	46.5	62.9	56.1	11.1
M1	Right	56.3	58.6	64.1	51.5	–
M2	Right	60.5	64.4	67.6	50.1	–
M3	Right	59.2	61.3	62.8	–	–

Table 2. Maxillary dentition measurements (mm) of the Berehove rhinoceros. DAP_0 antero-posterior dimension measured at the occlusal surface, *DAPb* antero-posterior dimension measured at the base of the crown, *DTa* transversal anterior dimension measured at the front of the crown, *DTp* transversal posterior dimension measured at the back of the crown, *HIi* distance between the lower crown border and the point where the lingual cusps' bases meet.

and shows only limited constriction, and the protocone–hypocone relationship is less integrated than in the Kvabebi material, where fusion of these elements is more pronounced in corresponding teeth. Enamel folding is present but less complex than in derived *Stephanorhinus* species. On P2, the ectoloph is convex with a strong parastyle, faint paracone and metacone ribs, and shallow crista and crochet undulations, but no antecrochet. The protocone, smaller than the hypocone, is only weakly connected to the ectoloph and was likely isolated early in wear. A lingual cingulum is absent or, if present, extremely weak and barely developed in the median valley. P3 and P4 show a similar pattern, with a fused protocone–ectoloph connection and a weakly expressed lingual cingulum. Unlike the Kvabebi material, no lingual cingulum or lingual folding is observed in the Berehove specimen. Dental wear indicates a young adult individual, comparable to a 15–20-year-old white rhinoceros or a 12–15-year-old black rhinoceros[38].

M1 bears a strong parastyle, a distinct paracone rib, a weak metacone rib and metastyle, and a robust crochet fused to the medifossette wall. No crista is visible. The protocone shows mesial/distal constrictions and an antecrochet. In M1 of the Berehove specimen, the protocone–hypocone bases appear fused; however, the degree of integration is less pronounced than in the Kvabebi material, and advanced wear obscures part of the lingual morphology. In contrast to the Kvabebi specimen, enamel folding is less complex, and lingual structures are more weakly expressed. The lingual cingulum on the upper molars is absent or extremely weak and barely developed in the median valley, consistent with the condition observed in the Kvabebi material. M2 shows a strong paracone rib, a clear parastyle, a weak metastyle, no metacone rib, and a robust crochet and crista, as well as an antecrochet. The medifossette is barely open, the protocone is less constricted than in M1, and the lingual cingulum is absent. M3 exhibits a weakly convex labial wall, a strong parastyle, a thick paracone rib, a robust crochet and crista, a nearly closed medifossette, no antecrochet, a large unconstricted protocone, and no lingual cingulum.

The combination of characters (in particular, the absence of crista and crochet on the relatively less worn P4, presence of robust crochet (and, on M2–M3, a crista) on the molars, and lack of lingual cingula on the upper molars) places the Berehove rhinoceros morphologically between earlier dicerorhinines sensu lato (e.g. "*Dihoplus*" *pikermiensis*, "*D.*" *ringstroemi*) and more derived *Stephanorhinus* species (e.g. *S. megarhinus*). However, advanced wear of the premolars and M1, combined with incomplete preservation of key ectoloph features, prevents a confident species-level diagnosis. The Berehove specimens are therefore regarded as undiagnostic and are only tentatively referred to *Scythicorhinus vekuai* gen. nov. et comb. nov., based on their metrical affinities, the absence of any character inconsistent with a basal *Coelodonta–Stephanorhinus* attribution, and the result of cladistic and phylogenetic analyses.

Phylogenetic analyses

The combined morphological–molecular analyses based on the expanded dataset recover a higher-level topology within Rhinocerotoidea that closely matches the results of Borrani et al.[22]. All three morphology-based analyses yielded congruent, well-resolved trees, with most clades supported by at least two methods (see Fig. 5 for the consensus, and Figs S1–S3 for the individual trees). Diceratheriinae, Aceratheriinae, Teleoceratinae, Elasmotheriinae, and Rhinocerotinae are each resolved as monophyletic, and the relationships among these clades are nearly identical to those reported in that study. *Uintaceras radinskyi* forms the sister lineage to Rhinocerotidae, with basal rhinocerotids such as *Trigonias*, and *Subhyracodon* diverging early, followed by a radiation of Eocene–Oligocene taxa and, subsequently, the crown-group subfamilies. Within Rhinocerotinae, two tribes are consistently recovered: Dicerotini (including *Ceratotherium*, *Diceros*, "*Dihoplus*" *pikermiensis*, "*D.*" *ringstroemi*, *Paradiceros* and *Shennongtherium*) and Rhinocerotini, which is subdivided into Rhinocerotina (*Gaindatherium*, *Lartetotherium*, *Nesorhinus*, *Rhinoceros*, and *Rusingaceros*) and Dicerorhinina (*Coelodonta*, *Dicerorhinus*, *Dihoplus*, and *Stephanorhinus*). The structure of Dicerorhinina, including the placement of *Stephanorhinus megarhinus*, *S. miguelcrusafonti*, and "*Dihoplus*" *ringstroemi*, is consistent with Borrani et al.[22] and is summarized only briefly here, as the focus lies on the Kvabebi rhinoceros.

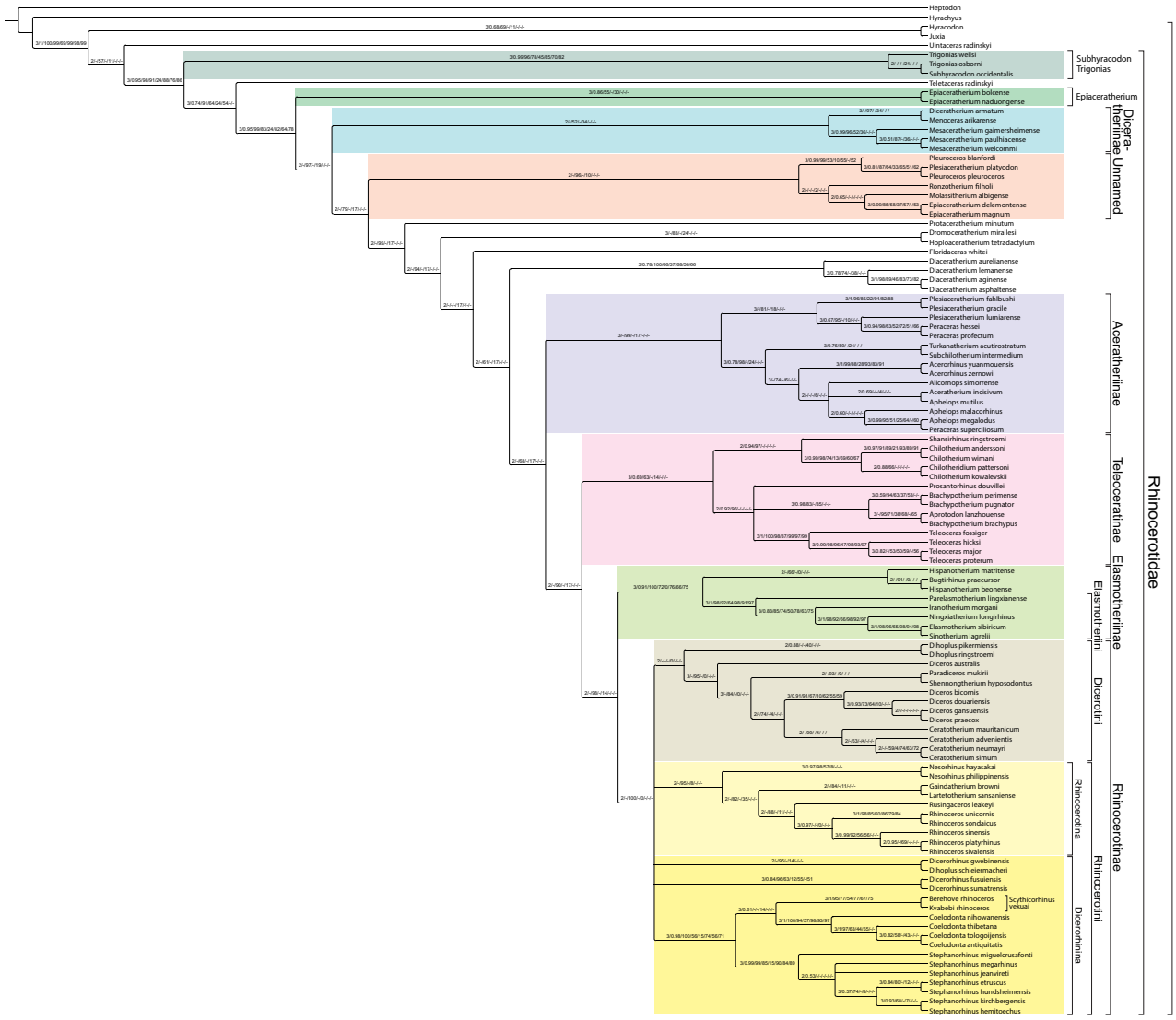

Fig. 5. Phylogenetic consensus tree inferred from morphological character data using three analytical approaches. Clades are color-coded according to synapomorphies and inferred relationships, including the calibrated tree. Node support values are shown as: (1) number of methods (out of three) supporting each clade; (2) posterior probabilities (MrBayes); (3) SH-aLRT and bootstrap (BS) values (IQ-TREE); (4) relative Bremer support, jackknife, BS, and symmetric resampling values (TNT). Posterior probabilities < 0.5 as well as jackknife, BS, and symmetric resampling values < 50% are shown by a dash ("–").

Across all analytical frameworks (maximum parsimony, maximum likelihood, and Bayesian inference), the Kvabebi rhinoceros was consistently recovered as the sister taxon to the Berehove specimen. This relationship received maximal or high support in all methods (Fig. 5), reinforcing the tentative referral of the Berehove material to *Scythicorhinus vekuai* gen. nov. et comb. nov. In the maximum-parsimony analysis, this pairing was supported by several synapomorphies, including: a premolar (P3–P4) to molar (M1–M3) row length ratio within the interval (42–50] (character 111); a long metastyl on M1 (character 190); absence of a lingual cingulum on M1 (character 202); a low and interrupted posterior cingulum on M1 (character 203); and absence of a posterior cingulum on M3 (character 233). All three analytical approaches placed the Kvabebi–Berehove clade as sister to the *Coelodonta* clade (Figs S1–S3). This placement was supported by seven synapomorphies: fusion of the protocone and hypocone bases on M1 (character 193); a mesiodistally oriented protoloph on M3 (character 224); a transversely (buccolingually) oriented metalophid on p2 (character 259); an angular, approximately right-angled trigonid on p4 (character 278); presence of a mesostyle on D3 (character 325) and D4 (character 326); and a quadrangular outline of the proximal facet of the scaphoid (character 417). Both the *Coelodonta* and *Stephanorhinus* were strongly supported under all three methods, and together with the Kvabebi–Berehove clade they formed a well-supported higher-level clade across all analyses (Fig. 5). This result contrasts with earlier classifications that referred the Kvabebi rhinoceros to *Stephanorhinus miguelcrusafonti*. Across all analytical methods, the Kvabebi material was consistently recovered as a lineage outside *Stephanorhinus* and closer to

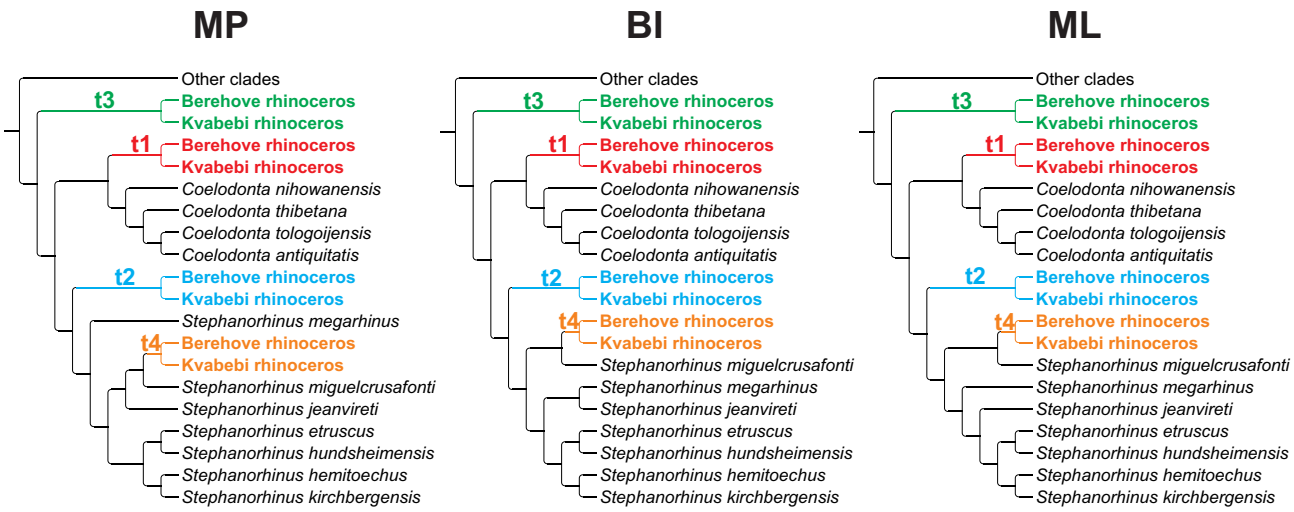

Topology	TL	TT	WST	BF	logL	bp-RELL	WSH	ELW	AU
t1	5991	-	-	-	-32084.9	0.467	0.770	0.461	0.621
t2	5992	0.782	1.000	0.73	-32085.4	0.387	0.844	0.382	0.633
t3	5996	0.096	0.180	1.05	-32088.2	0.115	0.510	0.124	0.230
t4	6010	0.005	0.007	7.03	-32100.6	0.032	0.081	0.033	0.045

Fig. 6. Preferred (t1) and alternative (t2, t3, t4) placements of the Kvabebi and Berehove rhinoceroses on maximum parsimony (MP), Bayesian Inference (BI), and maximum likelihood (ML) trees. The accompanying table reports tree length (TL); p-values from the Templeton test (TT) and Winning-sites (WST) tests; Bayes Factor (BF); log likelihood (logL); bootstrap proportion via RELL method (bp-RELL); and p-values from the weighted Shimodaira-Hasegawa (WSH), Expected Likelihood Weight (ELW), and approximately unbiased (AU) tests. BF are expressed as differences in log marginal likelihood relative to the best topology (t1). Values < 0.05 and BF > 3 are highlighted in red font. BF values of 1–3 indicate positive support, 3–5 strong support, and > 5 very strong support for the best tree[74].

Taxon	aCo	aSt	aSv/Co/St
Sv	22.1	23.3	16.4
Co	11.5	25.0	20.3
St	28.6	13.4	19.7

Table 3. The percent of different characters between the ancestors and considered taxa. Co – *Coelodonta*, Sc – *Scythicorhinus vekuai*, St – *Stephanorhinus*, a – common ancestor.

Coelodonta, never as sister to *S. miguelcrusafonti* (Fig. 5). In contrast, *S. miguelcrusafonti* was securely nested within *Stephanorhinus* in all analyses.

Under all three approaches, the Kvabebi–Berehove clade was placed as the sister group to *Coelodonta* (topology t1). Alternative topologies were evaluated, including: (1) placement within *Stephanorhinus* (topology t2), (2) placement basal to the *Coelodonta* + *Stephanorhinus* split (topology t3), and (3) a sister relationship to *S. miguelcrusafonti* (topology t4), corresponding to previous taxonomic assignments[13,14]. Although t1 was the best-supported topology, t2 and t3 were not significantly worse under the applied tests. Bayes Factor (BF) comparisons provided weak positive support for t1 over t2 and t3 (Fig. 6). In contrast, topology t4 was strongly rejected: BF and five tests yielded p-values < 0.05, while the wSH test returned p = 0.08, near the conventional threshold. Collectively, these results indicate that *Scythicorhinus vekuai* gen. nov. et comb. nov. occupies a position near the *Coelodonta–Stephanorhinus* divergence and, given its mosaic character combination, cannot be unambiguously assigned to either genus based on discrete-character distributions, morphometric distances, and alternative topology tests. A close relationship with *S. miguelcrusafonti* is unsupported, and assignment to either *Coelodonta* or *Stephanorhinus* at the species level is unwarranted. To assess the proximity of *Scythicorhinus vekuai* to the ancestral node uniting *Coelodonta* and *Stephanorhinus*, the proportion of character-state differences was compared between the reconstructed ancestor of the three lineages and the taxa considered, as well as between each taxon and the reconstructed ancestors of *Coelodonta* and *Stephanorhinus* (Table 3).

Scythicorhinus vekuai gen. nov. et comb. nov. differed by 16% from the reconstructed common ancestor of the three lineages, a lower value than observed for species of *Coelodonta* and *Stephanorhinus* (20%). In contrast, differences between *Scythicorhinus* and the reconstructed ancestors of *Coelodonta* and *Stephanorhinus* were higher (22–23%). Species of *Coelodonta* and *Stephanorhinus* differed less from their respective reconstructed ancestors (12–13%) than from species of the other genus (25–29%). This pattern is consistent with phylogenetic distances measured from the reconstructed ancestral node. In the Bayesian tree, the mean distance was 0.241 for *Scythicorhinus vekuai*, compared with 0.311 for *Stephanorhinus* and 0.355 for *Coelodonta*. In the maximum likelihood tree, the corresponding distances were 0.180 for *Scythicorhinus vekuai*, 0.255 for *Stephanorhinus*, and 0.256 for *Coelodonta*.

Distinction of Scythicorhinus vekuai from other taxa based on discrete characters

Phylogenetic analyses recover the Berehove and Kvabebi rhinoceroses as closely related taxa and place them near the divergence of *Coelodonta* and *Stephanorhinus*, but outside both genera as currently delimited. To further evaluate this pattern, the proportion of differing character states was compared among these taxa (Fig. 7). Species within each genus show similarly low levels of discrete-character divergence: 20–23% in *Coelodonta* and 19–29% in *Stephanorhinus*. In contrast, *Scythicorhinus vekuai* exhibits significantly higher proportions of different characters relative to both genera ($p < 0.044$), amounting to 31–36% when compared with *Coelodonta* and 29–36% when compared with *Stephanorhinus*. These largely overlapping values indicate that the Kvabebi and Berehove rhinoceroses are inconsistent with assignment to either genus. Moreover, these proportions are statistically indistinguishable ($p > 0.83$) from the 29–43% of characters separating *Coelodonta* and *Stephanorhinus*, as well as the 30–42% separating another closely related and well-defined generic pair, *Ceratotherium* and *Diceros*, including extant representatives. Accordingly, the morphological divergence of the Kvabebi and Berehove rhinoceroses from their nearest relatives is comparable to that observed among established rhinocerotid genera. The available material is therefore best interpreted as representing a distinct genus rather than a species within either *Coelodonta* or *Stephanorhinus*. A similar conclusion is supported by phylogenetic distances (Fig. 7). Distances between *Scythicorhinus vekuai* and *Coelodonta* or *Stephanorhinus* fall within the range observed between recognized genera (i.e., *Coelodonta–Stephanorhinus* and *Ceratotherium–Diceros*). Although the distance between *Coelodonta* and *Stephanorhinus* is the greatest ($p < 0.006$), distances involving *Scythicorhinus vekuai* are statistically indistinguishable from those separating *Ceratotherium–Diceros* distance ($p > 0.13$). In contrast, these distances are significantly greater than those observed at the species level within *Coelodonta* and within *Stephanorhinus* ($p < 0.004$).

Table S1 lists 26 characters that differ in state between the Kvabebi/Berehove rhinoceroses and more than half of the sampled species of *Coelodonta* and *Stephanorhinus*. Selected diagnostic characters are illustrated in Fig. 4. These characters highlight a set of features that contribute to the differentiation of *Scythicorhinus vekuai* from *Coelodonta* and *Stephanorhinus*. For example, the palatine surface (character 54) is concave in *Scythicorhinus vekuai*, whereas it is flat in all four species of *Coelodonta* and in six species of *Stephanorhinus* (*S. miguelcrusafonti* is coded as unknown). The aboral (posterior) margin of the mandibular symphyseal region (character 101) lies between p1 and p2 in *Scythicorhinus vekuai*, whereas in all *Coelodonta* species and in six *Stephanorhinus* species (*S. miguelcrusafonti* coded as unknown) it is positioned from beneath p2 to beneath p4, including intermediate positions between adjacent premolars. The P2 protoloph (character 141) and the M3 posterior cingulum (character 233) are absent in *Scythicorhinus vekuai* but present in all species of *Coelodonta* and in six species of *Stephanorhinus*. The lingual cingulum on M2 (character 220) is also absent in *Scythicorhinus vekuai* but present in all *Coelodonta* and all seven *Stephanorhinus* species. Finally, the entoconid on p2 (character 262) is absent in *Scythicorhinus vekuai* but present in three *Coelodonta* species (*C. tologoijensis* unknown) and in all seven *Stephanorhinus* species. With the exception of character 220, no other single character state unambiguously separates *Scythicorhinus* from both *Coelodonta* and *Stephanorhinus*; instead, its distinctiveness is supported by a unique combination of character states spanning cranial, dental, and postcranial morphology.

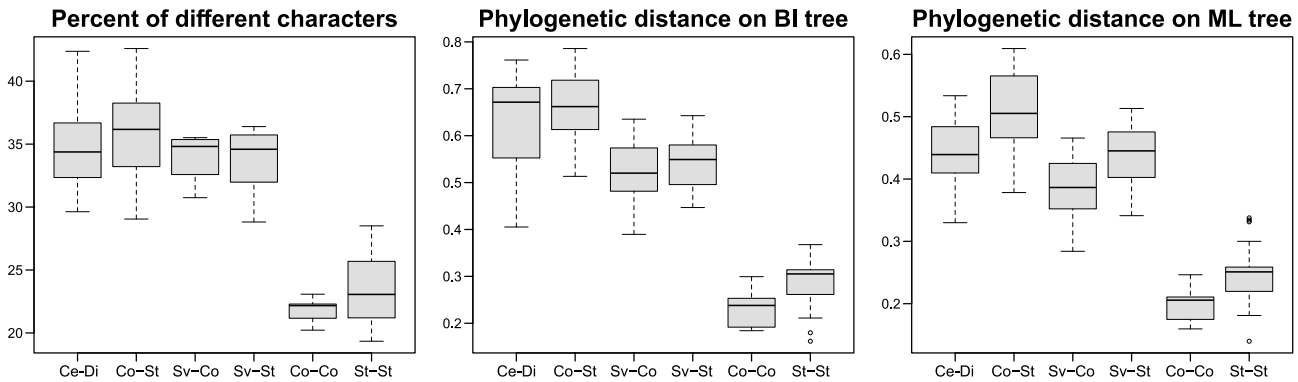

Fig. 7. Percentages of discrete character-state differences and phylogenetic distances (BI and ML trees) among selected rhinoceros taxa: Ce – *Ceratotherium*, Di – *Diceros*, Co – *Coelodonta*, Sv – *Scythicorhinus vekuai*, St – *Stephanorhinus*. Thick line: median; box: interquartile range; whiskers: range excluding outliers.

Analyses of morphometric data

Because phylogenetic analyses placed the Kvabebi and Berehove rhinoceroses near the *Coelodonta–Stephanorhinus* divergence, additional comparisons of dental and cranial measurements were conducted against representatives of both genera. Consistent with phylogenetic analyses indicating a close relationship between the Kvabebi and Berehove rhinoceroses and supporting their recognition as *Scythicorhinus vekuai* gen. nov. et comb. nov., comparisons of dental and cranial measurements indicate its clear differences from *Stephanorhinus* species, including *S. megarhinus* and *S. miguelcrusafonti* (Table S2). Mean values in *Scythicorhinus vekuai* gen. nov. et comb. nov. are consistently lower in all seven *Stephanorhinus* species, particularly for P4 length and width, p3 width, and cranial dimensions – c6 (distance from the postorbital process to the occiput), c9 (distance from the nasoincisive notch to the anterior rim of the orbit), c13 (distance from the posterior border of M3 to the posterior end of the occipital condyle on the same side), and c31 (width of the foramen magnum). Across the variables examined, values in *S. vekuai* gen. nov. et comb. nov. were on average 13% smaller (range 1.6–40.3%) than in *Stephanorhinus* species. Despite the limited sample size, several differences are statistically significant ($p = 0.037–0.004$): P4 and M1 are smaller than in *Stephanorhinus kirchbergensis*; M2 is longer and wider than in *S. etruscus*; M3 is wider than in *S. etruscus* and *S. hundsheimensis*; and occipital condyle width (c32) is smaller than in *S. kirchbergensis* and *S. megarhinus*. Hotelling's T^2 test of ten upper tooth variables indicates significant differences ($p = 0.018–0.0$) between *Scythicorhinus vekuai* gen. nov. et comb. nov. and *Stephanorhinus etruscus*, *S. hemitoechus*, *S. hundsheimensis*, and *S. kirchbergensis*.

Linear discriminant analysis (LDA) using five taxa and ten upper tooth variables shows clear species separation (Fig. 8A) with a 0.93 mean classification accuracy. Only *Stephanorhinus etruscus* and *S. hundsheimensis* show partial overlap, while *Scythicorhinus vekuai* gen. nov. et comb. nov. forms a distinct cluster. The first two discriminant functions (F1 and F2) explain 85% of variance. To interpret the biological relevance of the axes, structure coefficients were examined. F1 correlates negatively with L_M2 (-0.81), W_M3 (-0.67), L_P4 (-0.58), L_M3 (-0.56), W_M2 (-0.52), and W_M1 (-0.51); F2 correlates mainly with L_P2 (-0.21), L_P4 (0.22), and L_M3 (0.21).

Comparisons also reveal clear differences in craniodental measurements between *Scythicorhinus vekuai* gen. nov. et comb. nov. and *Coelodonta* (Table S2). The upper and lower teeth of *S. vekuai* exceed those of the four sampled *Coelodonta* species by an average of 10.2% (range: 0.4–27.1%) than those of the four sampled *Coelodonta* species, particularly P3, M2, M3, and p4 width, as well as p2, p3, p4, and m1 length. In contrast, cranial dimensions are on average 22.8% smaller (range: 4.4–40.3%) than those of the sampled *Coelodonta* species, most notably c9 (distance from the nasoincisive notch to the anterior rim of the orbit), c31 (foramen magnum width), and c32 (occipital condyle width). Statistically significant differences ($p = 0.01–0.001$) were detected between *S. vekuai* gen. nov. et comb. nov. and *C. antiquitatis* for c32 and for M2 and M3 width.

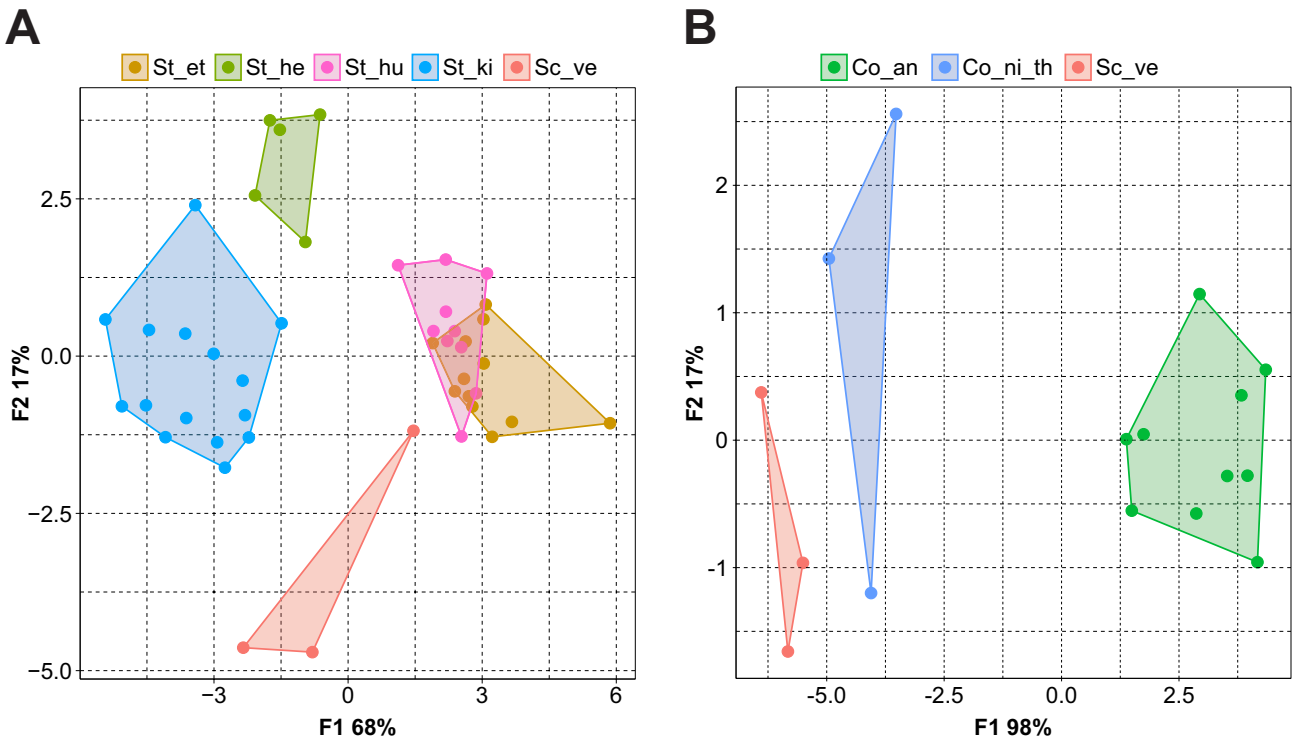

Fig. 8. LDA plot of *Scythicorhinus vekuai* (Sc_ve) compared with *Stephanorhinus* (**A**) and *Coelodonta* (**B**) species: *Stephanorhinus etruscus* (St_et), *S. hemitoechus* (St_he), *S. hundsheimensis* (St_hu), *S. kirchbergensis* (St_ki), *Coelodonta antiquitatis* (Co_an) and *C. nihowanensis* + *C. thibetana* (Co_ni_th). Percentages of variance explained by the first two discriminant functions (F1 and F2) are indicated.

Taxon 1	Taxon 2	Number of variables	Mean	Min	Max
Pliorhinus (Dri, Sme, Smi, Kva)	Set, She, Shu, Sje, Ski	7 for upper teeth, 9 for lower teeth	4.46	2.37	9.38
Pliorhinus (Dri, Sme, Smi, Kva)	*Pliorhinus* (Dri, Sme, Smi, Kva)		4.76	3.04	6.95
Set, She, Shu, Sje, Ski	Set, She, Shu, Sje, Ski		4.01	3.19	6.56
Kva	Smi	7 for upper teeth, 14 for lower teeth	3.59	–	–
Kva	Set, She, Shu, Sje, Ski, Sme		3.40	2.25	6.08
Smi	Set, She, Shu, Sje, Ski, Sme		3.45	2.48	4.61

Table 4. The normalized percentage difference $\overline{PD}$ between various groups of taxa. Dri – *Dihoplus. ringstroemi*; Kva – Kvabebi rhinoceros; Set – *S. etruscus*; She – *S. hemitoechus*; Shu – *S. hundsheimensis*; Sje – *S. jeanvireti*; Ski – *S. kirchbergensis*; Smi – *S. miguelcrusafonti*; Sme – *S. megarhinus*.

Hotelling's T^2 test based on eight upper-tooth variables also indicated significant differences between these taxa ($p = 0.011$). Clear separation between taxa was evident in the LDA based on eight upper-teeth variables (Fig. 8B). Mean classification accuracy was 0.94, and the first two discriminant functions explained 100% of the variance. *Scythicorhinus vekuai* gen. nov. et comb. nov. formed a distinct cluster near the combined group of *Coelodonta nihowanensis* and *C. thibetana*, whereas *C. antiquitatis* plotted more distantly. Structure coefficients indicated that F1 was most strongly (negatively) associated with W_M2 (-0.34), whereas F2 was most strongly associated with W_P4 (-0.40) and L_P4 (-0.25).

To assess distinctiveness in craniodental measurements relative to its closely related taxa (*Stephanorhinus* and *Coelodonta*), between-group variance (reflecting differences from the compared genus) and within-group variance (reflecting variation within that genus) were calculated for each variable. The substantial intraspecific variability documented for several *Stephanorhinus* species, particularly *S. kirchbergensis*, is explicitly accounted for through comparison of within-group and between-group variance. Due to limited sample sizes, *Coelodonta nihowanensis*, *C. thibetana*, and *C. tologoijensis* were combined into a single operational taxonomic unit, a grouping justified by their mutual similarity relative to *C. antiquitatis*. Among 43 craniodental variables compared with *Stephanorhinus* (243 variance comparisons), the mean between-group variance (299.9) significantly exceeded the mean within-group variance (132.5; $p = 1.23e-07$), averaging 6.5 times greater. In the *Coelodonta* dataset (27 variables), mean between-group variance (629.7) likewise exceeded mean within-group variance (147.4), averaging 7.9 times greater ($p = 0.001$). These results consistently support recognition of the Kvabebi/ Berehove material as a distinct taxon.

Given earlier classifications[13,21] placing *Stephanorhinus megarhinus*, *S. miguelcrusafonti,* and the Kvabebi rhinoceros in *Pliorhinus*, additional comparisons were conducted among these taxa and other *Stephanorhinus* species using mean normalized percentage difference ($\overline{PD}$) in craniodental measurements (Table 4). The resulting $\overline{PD}$ (4.46%) is lower than the intrageneric $\overline{PD}$ within *Pliorhinus* (4.76%) and only slightly higher than within *Stephanorhinus* (4.01%), offering no support for maintaining these taxa as generically distinct. Pandolfi et al.[13] assigned the Kvabebi rhinoceros to *Pliorhinus miguelcrusafonti*. Mean normalized $\overline{PD}$ were calculated between: (1) the Kvabebi rhinoceros and *Stephanorhinus miguelcrusafonti*; (2) the Kvabebi rhinoceros and other *Stephanorhinus* species (*S. etruscus*, *S. hemitoechus*, *S. hundsheimensis*, *S. jeanvireti*, *S. kirchbergensis*, and *S. megarhinus*); and (3) *S. miguelcrusafonti* and the same set of *Stephanorhinus* species (Table 4). Based on 21 dental measurements, the Kvabebi rhinoceros differs from *Stephanorhinus miguelcrusafonti* by 3.59%, which is slightly greater than its difference from the other *Stephanorhinus* species (3.40%) and also greater than the difference between *S. miguelcrusafonti* and these species (3.45%). These results contradict the proposed synonymy and do not support uniting the Kvabebi rhinoceros with *Stephanorhinus miguelcrusafonti*.

Discussion

The combined morphological, morphometric, and phylogenetic evidence presented here contributes to resolving several long-standing issues in the taxonomy of Eurasian rhinoceroses and provides a refined framework for interpreting the early diversification of the *Coelodonta* and *Stephanorhinus* lineage. The Kvabebi assemblage plays a central role in this reassessment. Its relative anatomical completeness for a Late Pliocene rhinoceros—encompassing cranial, mandibular, dental, and postcranial elements—permits a more comprehensive evaluation than has been possible in previous studies based on more limited material. Within the expanded phylogenetic framework applied here, the Kvabebi rhinoceros is consistently recovered as a distinct lineage within Dicerorhinina, positioned outside both *Coelodonta* and *Stephanorhinus* and close to their divergence.

However, alternative placements at the base of either genus are not statistically excluded, indicating that the precise phylogenetic position of this lineage remains sensitive to character sampling. This result highlights both the potential significance of the Kvabebi material and the need for caution in interpreting its systematic position.

The revised phylogenetic placement suggests that the earlier attribution of the Kvabebi material to *S. miguelcrusafonti* is not supported when evaluated within a broader comparative framework. Several morphological features—particularly in the upper dentition, mandibular structure, and postcranial elements—distinguish the Kvabebi rhinoceros from *S. miguelcrusafonti* and other species of *Stephanorhinus*. At the same time, the material does not exhibit the derived character states typical of *Coelodonta*. In particular, the absence of consistent hypsodonty and cement development, as well as differences in molar cingulum structure, make its direct assignment to *Coelodonta* problematic. Instead, it displays a combination of features that can be interpreted as intermediate or mosaic relative to both genera. Traditional diagnoses emphasized features such as the degree

of nasal septum ossification, reduction or loss of incisors (I2 and i2), hypsodonty, enamel complexity, and postcranial traits including metapodial elongation[1,13,37]. These characters were long regarded as stable indicators of generic affiliation[2,37,39]). Subsequent research, however, has shown that many are homoplasic, variably expressed across extinct and extant rhinocerotids, and often represent plesiomorphic conditions retained in early *Stephanorhinus*[1,12,13,37]. For example, incomplete nasal septum ossification and the persistence of small anterior incisors occur in early representatives of the genus, while increased enamel complexity and hypsodonty characterize more derived Pleistocene species such as *Stephanorhinus kirchbergensis* and *S. hemitoechus*. Similarly, several postcranial traits associated with cold-climate adaptations in the *Coelodonta* lineage appear only later in time[40]. Dietary and ecological studies further indicate substantial ecological variability among Pleistocene rhinocerotids[76-79]. Within this broader context, the character suite preserved in the Kvabebi material aligns well with expectations for an early representative of *Coelodonta–Stephanorhinus*.

Additional anatomical features reinforce this basal placement. Cranially, the shortened nasal notch–orbit distance and flattened temporal articular tubercle match conditions typical of *Stephanorhinus* and differ from those generally attributed to *Dihoplus*. The mandibular symphysis is ventrally flat in frontal view, again consistent with *Stephanorhinus*. The lower cheek teeth show complete fusion of the metaconid with a non-constricted metalophid on p4 and m1, a configuration characteristic of early *Stephanorhinus* and unlike earlier dicerorhinines. The upper cheek teeth display a gently curved lingual outline, a lingually open medifossette on P4, and a fused protocone–hypocone base on M1. Although brachydont, they exhibit complex enamel folding, a pattern absent in *Dihoplus schleiermacheri* and earlier dicerorhinines. The M-shaped proximal radius articulation, deep extensor groove on the ulna, tibial intercondyloid eminences of similar height, and astragalus with nearly equal proximal–distal extension of the medial and lateral lips all match *Stephanorhinus*. The calcaneus, with its elongate second facet and a low sustentaculum, further indicates this assignment. Taken together, these differences contradict the synonymy proposed by Pandolfi et al.[13,14] and support the recognition of *Scythicorhinus vekuai* as a distinct taxon.

This mosaic morphology is consistent with expectations for lineages close to the divergence of *Coelodonta* and *Stephanorhinus*, where homoplasy and retention of plesiomorphic characters complicate taxonomic assignments. Indeed, several characters traditionally used to distinguish dicerorhinine genera—such as enamel complexity, degree of hypsodonty, and aspects of cranial and postcranial morphology—are now recognized as variably expressed and, in some cases, homoplastic. Ecological studies have documented substantial variation in diet and habitat use among Eurasian rhinoceroses[76-78], while their chronology and geographic distribution have been in detail elsewhere[79]. In this context, the Kvabebi rhinoceros does not fit comfortably within existing generic diagnoses. Morphometric analyses further support this interpretation. The Kvabebi material consistently falls outside the range of variation observed in sampled species of both *Stephanorhinus* and *Coelodonta*, and statistical comparisons indicate that between-group differences exceed within-group variability in both genera. Although sample sizes are limited and some comparisons are affected by wear and preservation, these results are consistent with the hypothesis that the Kvabebi rhinoceros represents a distinct evolutionary lineage. On this basis, the recognition of *Scythicorhinus vekuai* is supported as a working taxonomic hypothesis that reflects both morphological distinctiveness and phylogenetic position. However, given the sensitivity of the topology to relatively minor changes in character scoring and the incompleteness of the available material, this assignment should be regarded as provisional. Future discoveries of more complete specimens and further refinement of phylogenetic datasets will be necessary to test the stability of this interpretation. The taxonomic implications of this reassessment extend to previously proposed generic frameworks. In particular, the present results support the rejection of *Pliorhinus* as a distinct genus. Consistent with recent phylogenetic analyses, the species previously included in *Pliorhinus* are more appropriately accommodated within *Stephanorhinus* or other dicerorhinine lineages, and do not form a monophyletic group. The Berehove material, although informative in documenting the presence of a large rhinocerotid in the northern Pontic region, remains insufficiently diagnostic at the species level due to advanced wear and fragmentary preservation. Its tentative referral to *Scythicorhinus vekuai* is supported by phylogenetic proximity and the absence of conflicting characters but should be considered provisional pending the discovery of more complete material.

Overall, the Kvabebi assemblage provides important evidence for the morphological diversity and phylogenetic complexity of Late Pliocene dicerorhinines. Rather than resolving all aspects of early *Coelodonta–Stephanorhinus* evolution, it highlights the existence of lineages that do not conform to established generic boundaries, emphasizing the need for continued revision of rhinocerotid systematics based on expanded datasets and integrative approaches.

Conclusions

This study resolves several long-standing taxonomic uncertainties within Eurasian Rhinocerotidae and provides new insight into the early evolution of *Coelodonta* and *Stephanorhinus*. Re-examination of the Kvabebi rhinoceros within an expanded morphological and phylogenetic framework indicates that it is interpreted as representing a distinct taxon, *Scythicorhinus vekuai* gen. nov. et comb. nov. Its anatomical features place it near the base of, but outside, the *Coelodonta* clade, thereby contributing to filling an important gap in the early diversification of this genus and related *Stephanorhinus*.

The broader comparative and phylogenetic context applied here shows that the criteria previously used to assign the Kvabebi rhinoceros to *Stephanorhinus miguelcrusafonti* are not supported when evaluated across cranial, dental, and postcranial character suites, nor under any analytical approach. Recognition of *Scythicorhinus vekuai* refines the diagnosis of early *Stephanorhinus* and helps resolve long-standing ambiguities surrounding taxa formerly placed in *Pliorhinus*. Consistent with recent phylogenetic studies, the results support the inclusion of *miguelcrusafonti* and *megarhinus* within *Stephanorhinus*, whereas "*Dihoplus*" *ringstroemi* is more appropriately positioned among basal Dicerotini. These findings reinforce the conclusion that *Pliorhinus* is not

monophyletic and should not be retained as a valid genus. Although too fragmentary and worn to contribute to the formal diagnosis, the Berehove maxillae show no morphological or phylogenetic conflict with *S. vekuai* and are therefore regarded as tentatively referable to the species. Together with the Kvabebi assemblage, they highlight the presence of early representatives of the lineage in Eastern Europe, suggesting a possible role of this region in its early diversification of *Coelodonta* and *Stephanorhinus* during the Late Miocene and Pliocene. More broadly, the phylogenetic placement of *S. vekuai* sheds light on the earliest stages of a lineage that later became a dominant component of Eurasian Pleistocene megafaunas. Its inferred evolutionary trajectory parallels major climatic changes during the late Neogene, underscoring the interplay between environmental dynamics and morphological innovation in rhinocerotid evolution. By integrating detailed morphological observations with expanded phylogenetic analyses, this study stabilizes *Stephanorhinus* taxonomy, clarifies interspecific relationships, and refines the broader evolutionary context of Eurasian rhinoceroses. The recognition of *Scythicorhinus vekuai* provides a stronger foundation for future research on the diversification and biogeography of the *Coelodonta–Stephanorhinus* clade.

Methods

Notations and terminology

This study follows standard cranial and dentognathic notation, morphological descriptors, and established terminology[1,37,41–44]. Upper teeth are indicated by capital letters (e.g. M1, M2, M3) and lower teeth by lowercase letters (e.g. m1, m2, m3). Deciduous teeth are denoted using a combination of uppercase and lowercase 'd'. The abbreviations Mc and Mt refer to metacarpal and metatarsal bones, respectively.

Morphological and morphometric analyses

The Berehove rhinoceros remains were identified using both morphological and morphometric criteria. Dental characters were compared with published descriptions[9,15,45–50], and measurements were taken with a 0.1 mm precision caliper following established protocols[37,43,44]. Individual age was estimated from dental wear patterns[38,51–53]. Three-dimensional scans of the specimens were produced using an Artec Space Spider scanner. Polygonal models were assembled in Artec Studio 15 Professional software and imported into Blender 2.91, where they were combined to reconstruct two virtual maxillae. The Kvabebi material forming the holotype and hypodigm of *Scythicorhinus vekuai* was comprehensively illustrated by Pandolfi et al.[13], who provided multi-view photographic documentation of all cranial, mandibular, dental, and postcranial elements. Because these figures depict the exact specimens re-examined in this study, and because the original fossils were available for direct inspection, no additional imaging was required. The morphological reassessment is based on first-hand examination, with the published illustrations serving as the permanent visual record of the type material.

Statistical analyses of morphometric data

Tooth and skull measurements (in mm) from four species of *Coelodonta*, seven species of *Stephanorhinus*, the Kvabebi rhinoceros, and "*Dihoplus*" *ringstroemi* were compiled from published sources (see references in the supplementary Excel file). Measurements expressed only as inequalities (e.g., less than or greater than a specific value) were excluded. Variables included the maximal length (L) and width (W) of upper and lower P2–P4 and M1–M3, as well as tooth-row lengths (premolars–molars, premolars only, last two premolars, and molars). Thirteen cranial measurements were also incorporated. The individual measurements were included in Tables S3, S4 and S5. Normality of each variable was tested using the Shapiro–Wilk test, and homogeneity of variances with Lévene's test. For pairwise comparisons, Welch's t-test was used when normality was satisfied; otherwise, the Wilcoxon-Mann–Whitney test was applied. For comparisons involving more than two groups, one-way Analysis of Variance (ANOVA) followed by Tukey's HSD test was used when assumptions were met; if not, the Kruskal–Wallis test followed by Dunn's post-hoc test was performed. A non-parametric two-sample Hotelling's T^2 test was used to compare groups across multiple variables, employing the James–Stein shrinkage estimator of Shaefer and Strimmer and 100,000 permutations. This approach was chosen after multivariate Shapiro–Wilk tests indicated deviation from normality. Between-group and within-group variances were calculated for *Scythicorhinus vekuai* relative to each species of *Stephanorhinus* and *Coelodonta*. Owing to the limited sample sizes and close similarity, *C. nihowanensis*, *C. thibetana*, and *C. tologoijensis* were combined into a single operational taxonomic unit (OTU). Differences between the two variance components were evaluated using a Wilcoxon-Mann–Whitney test, and p-values were adjusted for multiple comparisons using the Benjamini–Hochberg procedure. PERMANOVA (implemented in the R package *vegan*) was applied to distance matrices to test for differences in (1) the proportion of differing and (2) phylogenetic-tree distances between *Scythicorhinus vekuai* and other rhinoceros groups. Distance matrices were calculated using Euclidean distances; significance was assessed with 100,000 permutations, and p-values were adjusted using the Bonferroni correction. Statistical significance was set at $p < 0.05$. Linear Discriminant Analysis (LDA) was conducted on variables standardized using min–max normalization. For each taxon, the mean value m of each variable was calculated. The normalized percentage difference PD_v for each variable between two taxa was computed as follows:

$$PD_v = 100 * \frac{|m_1 - m_2|}{m_1 - m_2},$$

where m_1 and m_2 are the mean values for taxon 1 and 2, respectively.

The overall dissimilarity between taxa was expressed as the average of these values:

$$\overline{PD} = \frac{1}{n}\sum_{v=1}^{n} PD_v,$$

where n is the number of variables.

All statistical analyses were conducted in R v4.3.3 (R Core Team 2004; R Foundation for Statistical Computing, Vienna, Austria).

Phylogenetic analysis

Phylogenetic relationships were assessed using a matrix based on Borrani et al.[22], comprising 108 OTUs and 534 characters. Four genera were used as outgroups: *Heptodon* (Eocene tapiromorph), *Hyrachyus* (basal rhinocerotoid), *Juxia* (basal paraceratherid), and *Hyracodon* (hyracodontid) (Table S6). Additional details are provided in Table S7 and associated references. Character scoring for dicerorhinine taxa followed Borrani et al.[22] and was based on direct examination of specimens and published sources. Specimens examined first-hand included *Dicerorhinus sumatrensis*, *Stephanorhinus megarhinus*, *S. jeanvireti*, *S. etruscus*, *S. hundsheimensis*, *S. hemitoechus*, *S. kirchbergensis*, and *Coelodonta antiquitatis*. Additional scoring relied on the information provided particularly by Cerdeño[12], Antoine[1], Becker et al.[54], Tissier et al.[55], Wang[56], Deng et al.[57], Antoine et al.[58], Uzunidis et al.[59], and Lu et al.[60]. Analyses were conducted using three frameworks: Maximum Parsimony (MP) in TNT v1.6[61], Maximum Likelihood (ML) in IQ-TREE v2.3.4[62], and Bayesian Inference (BI) in MrBayes v3.2.7a[63]. Characters relating to p2 were scored exclusively on the basis of historical descriptions and illustrations[23,24], as this element is not preserved in the material currently available for direct examination. All such scorings were treated as uncertain where ambiguity existed.

All analyses incorporated topology constraints derived from a molecular phylogeny of Rhinocerotidae (Fig. S4, Table S8). A summary consensus tree was generated for visualisation only; evolutionary conclusions rely on the individual MP, ML, and BI topologies (provided in Figs S1–S3). In the MP analyses, all characters were treated as unordered. Three weighting schemes were applied: equal weighting, implied weighting, and extended implied weighting. For the latter two approaches, the K parameter (penalising homoplasy) was varied from 1 to 50. The optimal value ($K = 44$) was selected based on consistency index (CI), retention index (RI), and tree length (TL). Tree searches used the tree bisection and reconnection (TBR) algorithm with 100,000 replicates, retaining 10 trees per replicate. This algorithm produced only one most parsimonious tree. Branch support was assessed using relative Bremer support, jackknife resampling, bootstrap, and symmetric resampling (20,000 replicates each).

For ML analyses, ModelFinder[64] identified MK + FQ + R5 as the best-fitting morphological model based on the Bayesian Information Criterion (BIC). Tree searches used extensive nearest-neighbor interchange (NNI) optimization, starting from 1000 parsimony trees. The analysis terminated after 1000 unsuccessful iterations and included NNI optimization of the top 100 parsimony trees. The best tree with the largest maximum likelihood value was selected out of 30 such searches. Branch support was assessed using SH-like approximate likelihood ratio tests (SH-aLRT, 10,000 replicates) and non-parametric bootstrap analysis (2000 replicates).

In the BI analyses, a standard discrete morphological model with gamma-distributed rate heterogeneity (five categories) was used. Two independent runs of 96 Markov chains were performed, sampling every 100 generations for 100 million generations. A majority-rule posterior consensus tree was generated from the final 15.713 million generations, after confirming convergence via stabilization of the average standard deviation of split frequencies (< 0.01).

Alternative MP topologies were assessed in PAUP* 4.0a169[65] using the Templeton test[66] (Wilcoxon signed-rank test) and the winning-sites (sign) test. ML tree topologies were compared in IQ-TREE using 1 million RELL replicates and the following tests: bootstrap proportion (BP; RELL method[67]), weighted Shimodaira–Hasegawa (wSH) test[68], expected likelihood weights (ELW[69]), and the approximately unbiased (AU) test[70]. Competing BI topologies inferred in MrBayes were evaluated using Bayes Factors computed via stepping-stone sampling[71]. Mean marginal likelihoods were estimated from four independent runs (each with eight Markov chains), using 50 stepping-stone steps and 10,000,000 MCMC generations. Patristic distances for both BI and ML trees were calculated in Patristic[72] and MEGA software[73]. Ancestral states were reconstructed in PAUP* under the MP tree topology obtained in TNT.

Data availability

All data generated or analyzed during this study, including relevant input and output files used and produced in the phylogenetic analyses, are provided in the article and its Supplementary Information files.

Received: 13 October 2025; Accepted: 4 June 2026
Published online: 14 June 2026

References

1. Antoine, P. O. Phylogénie et évolution des Elasmotheriina (Mammalia, Rhinocerotidae). *Mém. Mus. natl. hist. nat. Paris* **188**, 1–353 (2002).
2. Fortelius, M. et al. Fossil mammals resolve regional patterns of Eurasian climate change over 20 million years. *Evol. Ecol. Res.* **4**, 1005–1016 (2002).
3. Eronen, J. T. et al. Precipitation and large herbivorous mammals I: estimates from present-day communities. *Evol. Ecol. Res.* **12**, 217–233 (2010).
4. Eronen, J. T. et al. Precipitation and large herbivorous mammals II: Application to fossil data. *Evol. Ecol. Res.* **12**, 235–248 (2010).

5. Pandolfi, L. Evolutionary history of Rhinocerotina (Mammalia, Perissodactyla). *Fossilia*, 27–32, https://doi.org/10.32774/FosRepPal.20.1810.102732 (2018).
6. Liu, S. et al. Ancient and modern genomes unravel the evolutionary history of the rhinoceros family. *Cell* **184**, 4874–4885. https://doi.org/10.1016/j.cell.2021.07.032 (2021).
7. Antoine, P. O., Becker, D., Pandolfi, L. & Geraads, D. Evolution and fossil record of Old World Rhinocerotidae. In *Rhinos of the World: Ecology, Conservation and Management* (eds Melletti, M. et al.) 31–48 (Springer Nature Switzerland, 2025).
8. Nardelli, F. & Heißig, K. A taxonomic review of the genus *Rhinoceros* with emphasis on the distinction of *Eurhinoceros* (Perissodactyla, Rhinocerotidae). *ZooKeys* **1230**, 303–333. https://doi.org/10.3897/zookeys.1230.127858 (2025).
9. De Christol, J. *Recherches sur les caractères des grandes espèces de rhinocéros fossiles* (J. Martel, 1834).
10. Thenius, E. Die Verknöcherung der Nasenscheidewand bei Rhinocerotiden und ihr systematischer Wert. (Zum Geschlechtsdimorphismus fossiler Rhinocerotiden). *Schweiz. Palaeont. Abh.* **71**, 1–17 (1955).
11. Fortelius, M., Mazza, P. & Sala, B. *Stephanorhinus* (Mammalia, Rhinocerotidae) of the western European Pleistocene, with a special revision of *Stephanorhinus etruscus* (Falconer, 1868). *Paleontogr. Ital.* **80**, 63–155 (1993).
12. Cerdeño, E. Cladistic analysis of the Family Rhinocerotidae (Perissodactyla). *Am. Mus. Novit.* **3143**, 1–25 (1995).
13. Pandolfi, L., Antoine, P.-O., Bukhsianidze, M., Lordkipanidze, D. & Rook, L. Northern Eurasian rhinocerotines (Mammalia, Perissodactyla) by the Pliocene-Pleistocene transition: Phylogeny and historical biogeography. *J. Syst. Palaeontol.* **19**, 1031–1057. https://doi.org/10.1080/14772019.2021.1995907 (2021).
14. Pandolfi, L., Sendra, J., Reolid, M. & Rook,. New Pliocene Rhinocerotidae findings from the Iberian Peninsula and the revision of the Spanish Pliocene records. *PalZ* **9**, 343–354. https://doi.org/10.1007/s12542-022-00607-9 (2022).
15. Guérin, C. & Santafe-Llopis, J. V. Dicerorhinus miguelcrusafonti nov. sp., une nouvelle espèce de rhinocéros (Mammalia, Perissodactyla) du gisement Pliocène supérieur de Layna (Soria, Espagne) et de la formation Pliocène de Perpignan (Pyrénées-Orientales, France). *Geobios* **11**, 457–491 (1978).
16. Pandolfi, L. & Rook, L. Rhinocerotidae (Mammalia, Perissodactyla) from the latest Turolian localities (MN 13; late Miocene) of central and northern Italy. *Bollettino della Società Paleontologica Italiana* **04**, 45–56. https://doi.org/10.4435/BSPI.2017.04 (2017).
17. Pandolfi, L., Rivals, F. & Rabinovich, R. A new species of rhinoceros from the site of Bethlehem: 'Dihoplus' bethlehemsis sp. Nov. (Mammalia, Rhinocerotidae). *Quat. Int.* **537**, 48–60. https://doi.org/10.1016/j.quaint.2020.01.011 (2020).
18. Cerdeño, E. Spanish Neogene rhinoceroses. *Palaeontology* **35**, 297–308 (1992).
19. Pandolfi, L., Marra, A. C., Carone, G., Maiorino, L. & Rook, L. A new rhinocerotid (Mammalia, Rhinocerotidae) from the latest Miocene of Southern Italy. *Hist. Biol.* **33**, 194–208. https://doi.org/10.1080/08912963.2019.1602615 (2021).
20. Pandolfi, L. *Sistematica e filogenesi dei Rhinocerotini (Mammalia, Rhinocerotidae)* (Dissertation, University of Rome, 2015).
21. Li, S., Sanisidro, O., Wang, S., Yang, R. & Deng, T. New materials of *Pliorhinus ringstroemi* from the Linxia Basin (Late Miocene, eastern Asia) and their taxonomical and evolutionary implications. *J. Mamm. Evol.* **31**, 6. https://doi.org/10.1007/s10914-023-09698-w (2024).
22. Borrani, A. et al. The evolutionary history of Rhinocerotidae: phylogenetic insights, climate influences, and conservation implications. *Cladistics* **42**, 46–62. https://doi.org/10.1111/cla.70015 (2026).
23. Vekua, A. *Kvabebi Fauna of Akchagylian Vertebrates*. Moscow, Nauka, 1–258 (1972).
24. Tsiskarishvili, G. V. 1987. *Late Tertiary Rhinoceroses (Rhinocerotidae) of Caucasus*. Tbilisi Metsniereba, 1–141 (1987).
25. Ratekhin, Y. O. The finding of a rhino in Pliocene deposits of the southwestern Crimea. *Visn. KDU Geol. Geogr.* **7**, 16–18 (1966).
26. Vernyhorova, Y. V. Stratigraphic scheme for the Neogene deposits of the Crimean Peninsula. *Heolohiia ta Rudonosnist Ukrainy* **2**, 59–106. https://doi.org/10.15421/121606 (2016).
27. *State Geological Map of Ukraine*. Scale 1:200 000. Crimean series. Sheets L-36-XXVIII (Evpatoriya), L-36-XXXIV (Sevastopol). State Geological Survey of Ukraine (2006).
28. Anistratenko, OYu. et al. Biostratigraphy of the Paleogene-Neogene deposits of the Alma Depression in Crimea. *Tecton. Stratigr.* **39**, 96–110. https://doi.org/10.30836/igs.0375-7773.2012.93140 (2012).
29. Veklych, M. F. *Paleostages and stratotypes of Upper Cenozoic soil formations*. Naukova dumka, Kyiv (1982).
30. Cohen, K. M., Finney, S. C., Gibbard, P. L. & Fan, J. X. The ICS International Chronostratigraphic Chart. *Episodes* **36**, 199–204 (2013).
31. Sokolov, N. A. *Mastodon arvernensis* and *Hipparion gracile* from Tertiary formations of the Crimea. *Tr. Sankt-Peterburgsk. Obshchestva Yestestvoispytatelei* **1**, 119–132 (1882).
32. Lysenko, N. I. On the new find of hipparion in the Pliocene of the Crimea. *Paleontol. Zhurn.* **3**, 139–140 (1960).
33. Lysenko, M. I. Mastodon (Tetralophodon aff. longirostris Caup) from Pliocene deposits of the Crimea. *Zbirn. prats Zool. muz. AN URSR* **31**, 52–55 (1962).
34. Kaiser, T. M., Brasch, J., Castell, J. C., Schulz, E. & Clauss, M. Tooth wear in captive wild ruminant species differs from that of free-ranging conspecifics. *Mamm. Biol.* **74**(425–437), 2009. https://doi.org/10.1016/j.mambio.2008.09.003 (2009).
35. Lazarev, S. From the Eastern Paratethys to the Pontocaspian basins: Late Miocene–Middle Pleistocene magneto-biostratigraphy, sedimentary architecture and faunal turnovers of the shrinking basins of West Eurasia. PhD dissertation, Utrecht University (2020).
36. Guérin, C. & Santafé-Llopis, J. V. Dicerorhinus miguelcrusafonti nov. sp., une nouvelle espèce de rhinocéros (Mammalia, Perissodactyla) du gisement pliocène supérieur de Layna (Soria, Espagne) et de la formation pliocène de Perpignan (Pyrénées-Orientales, France). *Geobios* **11**, 457–491. https://doi.org/10.1016/S0016-6995(78)80080-1 (1978).
37. Guérin, C. Les rhinocéros (Mammalia, Perissodactyla) du Miocène terminal au Pléistocène supérieur en Europe occidentale. Comparaison avec les espèces actuelles. *Docum. Lab. Géol. Lyon* **79**, 3–1183 (1980).
38. Hillman-Smith, A. K. K., Owen-Smith, N., Anderson, J. L., Hall-Martin, A. J. & Seladi, J. P. Age estimation of the White rhinoceros (*Ceratotherium simum*). *J. Zool.* **210**, 355–377. https://doi.org/10.1111/j.1469-7998.1986.tb03639.x (1986).
39. Heissig, K. Family Rhinocerotidae. In *The Miocene Land Mammals of Europe* (eds Rössner, G. E. & Heissig, K.) 175–188 (Verlag Dr. Friedrich Pfeil, 1999).
40. Deng, T. et al. Out of Tibet: Pliocene woolly rhino suggests high-plateau origin of Ice Age megaherbivores. *Science* **333**, 1285–1288. https://doi.org/10.1126/science.1206594 (2011).
41. Pandolfi, L., Gasparik, M. & Piras, P. Earliest occurrence of "*Dihoplus*" *megarhinus* (Mammalia, Rhinocerotidae) in Europe (late Miocene, Pannonian Basin, Hungary): palaeobiogeographical and biochronological implications. *Ann. Paléontol.* **101**, 325–339. https://doi.org/10.1016/j.annpal.2015.09.001 (2015).
42. Lacombat, F. Les rhinocéros fossiles des sites préhistoriques de l'Europe méditerranéenne et du Massif Central. *Paléontologie et implications bio-chronologiques. BAR Int. Ser* 1419 (2005).
43. Lacombat, F. Morphological and biometrical differentiation of the teeth from Pleistocene species of *Stephanorhinus* (Mammalia, Perissodactyla, Rhinocerotidae) in Mediterranean Europe and the Massif Central. *France. Palaeontogr. Abt. A* **274**, 71–111 (2006).
44. Lacombat, F. Pleistocene Rhinoceroses in Mediterranean Europe and in Massif Central (France). *Cour. Forsch.-Inst. Senckenberg* **256**, 57–69 (2006).
45. Falconer, H. On the species of fossil Rhinoceros found in the Sewalik Hills and On the fossil Rhinoceros of central Tibet and its relation to the recent upheaval of the Himalayahs in *Palaeontological Memoirs and Notes of the late Hugh Falconer* (ed. C. Murchison) (1868).
46. Sacco, F. Le rhinocéros de Dusino (Rhinoceros etruscus Falc., var. astensis Sacc.). *Arch. Mus. Hist. Nat. Lyon* **6**, 1–31 (1895).
47. Sacco, F. Resti fossili di Rinoceronti dell'Astigiana. *Mem. Reg. Accad. Sci. Torino* **2**, 105–116 (1906).

48. Simonelli, V. I Rinoceronti fossili del museo di Parma. *Palaeontogr. Ital.* **3**, 89–136 (1897).
49. Guérin, C., Ballesio, R. & Méon, H. L. Dicerorhinus megarhinus (Mammalia, Rhinocerotidae) du Pliocène de Saint-Laurent-des-Arbres (Gard). *Docum. Lab. Géol. Lyon* **31**, 55–145 (1969).
50. Guérin, C. Etude de nouveaux restes de vertébrés provenant de la carrière Fournier à Châtillon-Saint-Jean II. *Rhinocéros. Bull. Assoc. Franç. Quatern.* **9**, 263–270 (1972).
51. Hitchins, P. M. Age determination of the black rhinoceros, *Diceros bicornis* Linn. *Zululand. South Afr. J. Wildl. Res.* **8**, 71–80 (1978).
52. Kirillova, I. V. & Shidlovskiy, F. K. Estimation of individual age and season of death in woolly rhinoceros, *Coelodonta antiquitatis* (Blumenbach, 1799), from Sakha-Yakutia. *Russia. Quat. Sci. Rev.* **29**, 3106–3114. https://doi.org/10.1016/j.quascirev.2010.06.036 (2010).
53. Taylor, L. A. et al. Detecting inter-cusp and inter-tooth wear patterns in Rhinocerotids. *PLoS ONE* **8**, e80921. https://doi.org/10.1371/journal.pone.0080921 (2013).
54. Becker, D., Antoine, P. O. & Maridet, O. A new genus of Rhinocerotidae (Mammalia, Perissodactyla) from the Oligocene of Europe. *J. Syst. Palaeontol.* **11**(947–972), 2013. https://doi.org/10.1080/14772019.2012.699007 (2013).
55. Tissier, J., Antoine, P. O. & Becker, D. New material of *Epiaceratherium* and a new species of *Mesaceratherium* clear up the phylogeny of early Rhinocerotidae (Perissodactyla). *R. Soc. Open Sci.* **7**, 200633. https://doi.org/10.1098/rsos.200633 (2020).
56. Wang, B. *Reconstructing the paleoecology and biogeography of rhinoceroses (Mammalia: Rhinocerotidae) in the Great Plains of North America, leading up to their extinction in the Early Pliocene* (Thesis (Department of Earth and Atmospheric Sciences, University of Nebraska-Lincoln, 2016).
57. Deng, T. et al. An Oligocene giant rhino provides insights into *Paraceratherium* evolution. *Commun. Biol.* **4**, 639. https://doi.org/10.1038/s42003-021-02170-6 (2021).
58. Antoine, P. O. et al. A new rhinoceros clade from the Pleistocene of Asia sheds light on mammal dispersals to the Philippines. *Zool. J. Linn. Soc.* **194**, 416–430. https://doi.org/10.1093/zoolinnean/zlab009 (2022).
59. Uzunidis, A., Antoine, P. O. & Brugal, J. P. A Middle Pleistocene *Coelodonta antiquitatis praecursor* Guérin (1980) (Mammalia, Perissodactyla) from Les Rameaux, SW France, and a revised phylogeny of *Coelodonta* Bronn, 1831. *Quat. Sci. Rev.* **288**, 107594. https://doi.org/10.1016/j.quascirev.2022.107594 (2022).
60. Lu, X. K., Deng, T. & Pandolfi, L. Reconstructing the phylogeny of the hornless rhinoceros Aceratheriinae. *Front. Ecol. Evol.* **11**, 1005126. https://doi.org/10.3389/fevo.2023.1005126 (2023).
61. Goloboff, P. A. & Morales, METNTversion16. TNT version 1.6, with a graphical interface for MacOS and Linux, including new routines in parallel. *Cladistics* **12524**, 144–153. https://doi.org/10.1111/cla.12524 (2023).
62. Nguyen, L. T., Schmidt, H. A., Von Haeseler, A. & Minh, B. Q. IQ-TREE: a fast and effective stochastic algorithm for estimating maximum-likelihood phylogenies. *Mol. Biol. Evol.* **32**, 268–274. https://doi.org/10.1093/molbev/msu300 (2015).
63. Ronquist, F. et al. MrBayes 3.2: Efficient Bayesian phylogenetic inference and model choice across a large model space. *Syst. Biol.* **61**, 539–542. https://doi.org/10.1093/sysbio/sys029 (2012).
64. Kalyaanamoorthy, S., Minh, B. Q., Wong, T. K., Von Haeseler, A. & Jermiin, L. S. ModelFinder: fast model selection for accurate phylogenetic estimates. *Nat. Methods* **14**, 587–589. https://doi.org/10.1038/nmeth.4285 (2017).
65. Swofford, D. L. Phylogenetic analysis using parsimony (*and other methods). Version 4. Sinauer Associates, Sunderland, Massachusetts (2003).
66. Templeton, A. R. Phylogenetic inference from restriction endonuclease cleavage site maps with particular reference to the evolution of humans and apes. *Evolution* **37**, 221–244. https://doi.org/10.1111/j.1558-5646.1983.tb05533.x (1983).
67. Kishino, H., Miyata, T. & Hasegawa,. Maximum likelihood inference of protein phylogeny and the origin of chloroplasts. *J. Mol. Evol.* **31**, 151–160. https://doi.org/10.1007/BF02109483 (1990).
68. Shimodaira, H. & Hasegawa,. Multiple comparisons of log-likelihoods with applications to phylogenetic inference. *Mol. Biol. Evol.* **16**, 1114–1116. https://doi.org/10.1093/oxfordjournals.molbev.a026201 (1999).
69. Strimmer, K. & Rambaut,. Inferring confidence sets of possibly misspecified gene trees. *Proc. R. Soc. Lond. B Biol. Sci.* **1862**, 137–142. https://doi.org/10.1098/rspb.2001.1862 (2002).
70. Shimodaira,. An approximately unbiased test of phylogenetic tree selection. *Syst. Biol.* **51**, 492–508. https://doi.org/10.1080/10635150290069913 (2002).
71. Baele, G. et al. Improving the accuracy of demographic and molecular clock model comparison while accommodating phylogenetic uncertainty. *Mol. Biol. Evol.* **29**, 2157–2167. https://doi.org/10.1093/molbev/mss084 (2012).
72. Fourment, M. & Gibbs, M. J. PATRISTIC: A program for calculating patristic distances and graphically comparing the components of genetic change. *BMC Evol. Biol.* **6**, 1. https://doi.org/10.1186/1471-2148-6-1 (2006).
73. Tamura, K., Stecher, G. & Kumar,. MEGA11: Molecular Evolutionary Genetics Analysis version 11. *Mol. Biol. Evol.* **38**, 3022–3027. https://doi.org/10.1093/molbev/msab120 (2021).
74. Kass, R. E. & Raftery, A. E. Bayes Factors. *J. Am. Stat. Assoc.* **90**, 773–795. https://doi.org/10.1080/01621459.1995.10476572 (1995).
75. ICZN. International Code of Zoological Nomenclature. Fourth Edition. London, UK: The International Trust for Zoological Nomenclature (1999).
76. Rivals, F., Schulz, E. & Kaiser,. Late and middle Pleistocene ungulates dietary diversity in Western Europe indicate variations of Neanderthal paleoenvironments through time and space. *Quat. Sci. Rev.* **004**, 3388–3400. https://doi.org/10.1016/j.quascirev.2009.09.004 (2009).
77. van Asperen, E. N. & Kahlke, R. D. Dietary variation and overlap in Central and Northwest European *Stephanorhinus kirchbergensis* and *S. hemitoechus* (Rhinocerotidae, Mammalia) influenced by habitat diversity: "You'll have to take pot luck!" (proverb). *Quat. Sci. Rev.* **107**(1), 47–61. https://doi.org/10.1016/j.quascirev.2014.10.001 (2015).
78. Stefaniak, et al. Browsers, grazers or mix-feeders? Case study of the diet of extinct Eurasian rhinos of the genus *Stephanorhinus* (Kretzoi, 1942) and the woolly rhinoceros *Coelodonta antiquitatis* (Blumenbach, 1799). *Quat. Int.* **605–605**, 192–212. https://doi.org/10.1016/j.quaint.2020.08.039 (2021).
79. Stefaniak, K. et al. Chronology and distribution of Central and Eastern European Pleistocene rhinoceroses (Perissodactyla, Rhinocerotidae) – A review. *Quat. Int.* **674–675**, 87–108. https://doi.org/10.1016/j.quaint.2023.02.004 (2023).

Acknowledgements

The authors extend their sincere thanks to S. Dominici, L. Bellucci, and A. Savorelli for providing access to rhinoceros specimens housed in the Paleontology Section of the Museum of Natural History, University of Florence (Italy), enabling direct examination of the material. A.B. also thanks superintendent A. Betori (Soprintendenza Archeologia, Belle Arti e Paesaggio per le Province di Frosinone e Latina) for his kind support. P.P.A.M. was supported in the present study by the PAULMAZZARICATEN26—Mazza P. Fondo Ateneo 2026 MUR (Italian Ministry of Universities and Research) grant, as well as by the Institutional Recognition (Art. 4, para. 2 of Call 2025) awarded by the Ministry of Foreign Affairs and International Cooperation (MAECI) to project Arc-3089. We further wish to thank three anonymous reviewers for their insightful comments and helpful suggestions that significantly improved the manuscript.

Author contributions

O.K., A.B., P.P.A.M., and K.S. conceived the study and coordinated the research. Paleontological analysis of the rhinoceros fossils was carried out by O.K., A.B., K.S., C.C., U.R.-S., and Z.B.; C.C. focused specifically on dental microstructure. Cladistic analyses were performed by A.B., P.M., and M.S., with P.M. also conducting the phylogenetic interpretation based on molecular evidence. P.M. carried out the statistical analyses of morphometric and discrete data; S.D. photographed the specimens and produced the 3D models. A.D. prepared Fig. 1 and drawings of the Berehove specimens, which were used by M.S. for the skull reconstruction. The manuscript was written by P.P.A.M., A.B., O.K., P.M., and K.S., with all co-authors contributing through comments and revisions.

Funding

This research was partly supported by the PAULMAZZARICATEN24 – Mazza P. Fondo Ateneo 2024 grant from MIUR (Italian Ministry of Education, Universities, and Research), which funded P.P.A.M.'s contribution. Additional support was provided by the National Academy of Sciences of Ukraine (0125U000927, 0124U000572) for O.K. and A.D. as well as by subsidy 2025; (501); MPK 2599280000 ZP; discipline 73 awarded to K.S. and U.R.S. Computational analyses were partly conducted using resources provided by the Wrocław Center for Networking and Supercomputing (grant No. 307 and 442).

Declarations

Competing interests

The authors declare no competing interests.

Additional information

Supplementary Information The online version contains supplementary material available at https://doi.org/10.1038/s41598-026-57113-0.

Correspondence and requests for materials should be addressed to O.K.

Reprints and permissions information is available at www.nature.com/reprints.

Publisher's note Springer Nature remains neutral with regard to jurisdictional claims in published maps and institutional affiliations.